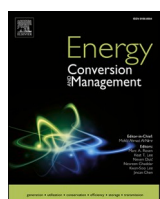
ELSEVIER

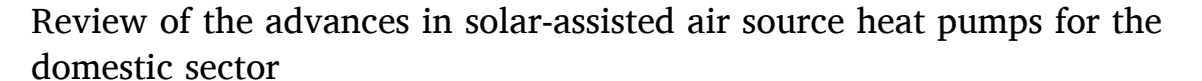
Contents lists available at ScienceDirect

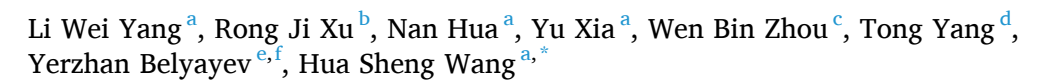
Energy Conversion and Management

journal homepage: www.elsevier.com/locate/enconman



Review





- ^a School of Engineering and Materials Science, Queen Mary University of London, Mile End Road, London E1 4NS, UK
- ^b Beijing University of Civil Engineering and Architecture, Beijing 100044, China
- ^c Department of Mechanical Engineering, Imperial College London, London SW7 2AZ, UK
- d Faculty of Science and Technology, Middlesex University, London NW4 4BT, UK
- e Department of Mechanical Engineering and Modeling, Satbayev University, 22a Satbayev Street, Almaty 050013, Kazakhstan
- f Department of Mechanics, Al-Farabi Kazakh National University, 71 Al-Farabi Avenue, Almaty 050040, Kazakhstan

ARTICLE INFO

Keywords: Solar-assisted air source heat pump Coefficient of performance System configuration Solar collector Thermal energy storage Defrosting

ABSTRACT

Solar assisted air source heat pump shows great potential as a promising energy-saving heating technology, which integrates solar collector and air source heat pump. It is widely considered for supplying hot water, space heating and/or space cooling in the domestic sector. The performance of solar assisted air source heat pumps can be evaluated in system level by parameters such as coefficient of performance, seasonal performance factor, energy consumption, solar fraction as well as initial and operating costs, and in component level by parameters such as efficiencies of solar collection and thermal energy storage. Their performances are affected by many factors such as system configuration, components size, working fluid, working conditions and weather conditions. This paper presents a comprehensive review on the recent advances in solar assisted air source heat pump for the domestic sector in terms of system configuration, solar collectors, thermal energy storage, defrosting method and the perspective areas of further investigations. The results of this review confirm that research is still required to improve the performance of such a combined system and reduce initial cost compared with existing heating systems based on hydrocarbon combustion. The information presented in this paper is beneficial to the researchers, small and medium-sized enterprises suppling renewable energy system technologies, heating engineers and service workers, energy policy and decision makers, environmental activists and communities.

1. Introduction

Heat pumps (HPs) can be considered as both energy efficient and renewable energy technology [1]. The use of this technology to increase buildings energy efficiency by utilizing low-grade thermal energy from existing heating supply systems is of significant interest today. However, to significantly reduce energy consumption and to improve the performance of HPs, many studies are devoted to increasing the share of renewable energy. According to the International Energy Agency (IEA), worldwide, thermal energy accounts for more than 50% of energy consumption, with about 45% consumed in residential and commercial buildings [1]. In the UK, heating took up 48% of the total energy consumption in 2013, and the domestic sector accounted for 57% of the entire heating demand [2]. Emissions of greenhouse gases (GHGs) and

air pollutants during heat provision from hydrocarbon combustion are 39%, with fossil fuel being the main heat source today [1]. To achieve the UK's target of the net-zero emissions of GHGs by 2050, the domestic heating sector has to be decarbonised [3]. Many countries have a strategy by 2050 to increase the share of renewable energies. In combination with renewable energy, an increase in HPs in heating provision is expected. By 2030, HP should provide 22.1% of the domestic heating compared with 5% in 2019 [1]. The coefficient of performance (*COP*) and seasonal performance factor (*SPF*) are parameters to evaluate the performance of HPs [4]. HPs are divided into air source heat pump (ASHP), ground source heat pump (GSHP), water source heat pump (WSHP) and soar assisted heat pumps (SAHP). Depending on the purpose of application, climate conditions, technical and economic parameters, each of them has its own advantages and disadvantages.

Table 1 lists of review papers on solar-assisted ASHPs (SAASHPs,

E-mail address: h.s.wang@qmul.ac.uk (H.S. Wang).

0196-8904/© 2021 Elsevier Ltd. All rights reserved.



^{*} Corresponding author.

Nomeno	clature	Greek Let	tters:
		$\eta_{ m sc}$	efficiency of solar collector
A	area, m ²	ρ	density of air, kg/m ³
	area, m ² coefficient of performance specific heat capacity, J/(kg K) average amount of energy received per square meter of a solar collector, W/m ² heating capacity, W average monthly value of atmosphere lucidity heat pump heating capacity, W heating demand, W heat loss, W maximum thermal energy storage capacity, J thermal energy collected by a solar collector, W solar fraction (solar heating ability) seasonal performance factor time, s ambient air temperature, °C condensing temperature, °C temperature of storage tank fully-charged, °C temperature of storage tank fully-discharged, °C water/refrigerant temperature at the inlet of solar	η _{sc} ρ Abbreviat ASHP DX-SAAS GHG GSHP GWP HP HW IEA	efficiency of solar collector density of air, kg/m³ ion: air source heat pump HP direct expansion solar-assisted air source heat pump greenhouse gases ground source heat pump global warming potential heat pump hot water International Energy Agency HP indirect expansion solar-assisted air source heat pump ozone depletion potential phase change material photovoltaic photovoltaic/thermal solar-assisted air source heat pump
l		SC	space cooling
1 sc,in	collector, °C	SFH	single family house
V	volume, m ³	SH	space heating
$W_{\rm com}$	work done by compressor, W	SWH	solar water heater
W_{fan}	work done by fan, W	TES	thermal energy storage
$W_{ m pump}$	work done by pump, W	VFD	variable frequency drive
$W_{ m tot}$	total work done by compressor, fans, pumps, W	WSHP	water source heat pump

vapour-compression HPs). Two approaches to solar boosting that have reported are direct expansion SAASHP (DX-SAASHP) [5-9] and indirect expansion SAASHP (IX-SAASHP) [10-23]. In the DX-SAASHPs, refrigerant is circulated directly through the solar collectors which serve as the HP evaporator. Investigations on DX-SAASHPs were devoted to exergy analyses, performance evaluation of the entire system and individual components, refrigerants, component and system modelling, solar thermal collector modelling, optimal design and control, various applications such as hot water (HW) provision, space heating (SH), drying, desalination, vaporisation of liquid fuels. From these reviews, further trends were identified such as the use of DX-SAASHP for space cooling (SC), developing highly efficient/low-cost/building-integrated collector-evaporator, establishing DX-SAASHP standardization for the design/production and assembling, and exploring optimal control strategies. DX-SAASHPs have not been widely used compared with IX-SAASHPs. In IX-SAASHPs, an intermediate heat transfer fluid is circulated through the solar collectors and the installation is simplified but requiring an additional heat exchanger. An IX-SAASHP performs better than either ASHP [24] or solar heating [25]. For example, application of serial IX-SAASHP in Canadian domestic sector reduced GHG emission by 19% [26]. The use of an air source evaporator in addition to a solar collector allows extracting heat from the ambient air when solar radiation is not available, which expands the capability of the system. However, there is an issue of frost formation of the outdoor unit when the ambient air temperature is below zero, especially in humid regions. The COP and SPF of the system can be improved by integrating thermal energy storage (TES) [27,28]. Reviews on IX-SAASHPs focused on types of solar collectors including photovoltaic/thermal, energy and exergy analyses, components modelling, environment-friendly refrigerants, system performance and efficiency parameters, hydraulics and control, mathematical modelling approaches (artificial neural networks, life cycle assessment, TRNSYS, etc.), improvement in cycle design (cascade cycle, ejector enhanced cycle, etc.), different applications (SH, drying, desalination, etc.), and market and economic analyses.

Many theoretical, numerical simulations and experimental studies on SAASHP have been conducted in recent years. The utilization of SAASHP for HW and/or SH as well as SC has shown great achievements in decarbonization of heating and cooling. So far, few comprehensive reviews have focused on recent advances in SAASHPs for the use in domestic sector. This paper was motivated to thoroughly review the research developments in SAASHPs for domestic heating. This paper aims at providing a comprehensive review on the state-of-the-art of SAASHPs. Fig. 1 summarizes the framework of this review paper. This review is structured in such a way that the influence of three key components: solar thermal collectors, TES (sensible and latent heats) and air source evaporator including defrosting methods.

2. Design of solar-assisted air source heat pumps

SAASHPs (see Table 2) include DX-SAASHP, IX-SAASHP and hybrid systems. In the DX-SAASHPs, the solar collector serves as an evaporator whereas in the IX-SAASHPs, a heat exchanger connects the refrigerant and water loops. The DX-SAASHPs mainly include basic and dual-source DX-SAASHPs. Compared with basic DX-SAASHP, the dual-source DX-SAASHP has an extra air source heat exchanger [29]. The IX-SAASHPs mainly include serial and dual-source systems. In the IX-SAASHPs, a heat exchanger is used to transfer heat from the solar collector to refrigerant. In the hybrid system, an ASHP is parallel to the solar HW loop. Some special SAASHPs have been studied, such as two-stage DX-SAASHP, vapour ejector-enhanced DX-SAASHP, auto-cascade IX-SAASHP, composite IX-SAASHP and trans-critical hybrid system.

The performance of SAASHP is evaluated by *COP*, *SPF* and solar fraction (*SF*). *COP* is defined by Eq. (1) [30]

$$COP = Q_{\rm co}/W_{\rm tot} \tag{1}$$

where Q_{co} is the heating capacity and W_{tot} is the total work done by the compressor, fans and pumps given by Eq. (2)

$$W_{\text{tot}} = W_{\text{fan}} + W_{\text{com}} + W_{\text{pump}} \tag{2}$$

SPF is the seasonal performance factor that evaluates the efficiency over the whole heating season, the ratio of the total thermal energy delivered by the SAASHP to the total electric energy consumed by compressor, pump and fan, given by Eq. (3).

$$SPF = \int Q_{\rm co} dt / \int W_{\rm tot} dt \tag{3}$$

where *t* is time.

The SF is the solar fraction defined by Eq. (4) [31]

$$SF = (Q_{\rm sc} - -Q_{\rm loss})/Q_{\rm hd} \tag{4}$$

where $Q_{\rm sc}$ is the average amount of thermal energy collected by a solar collector, $Q_{\rm loss}$ is the heat loss of the system and $Q_{\rm hd}$ is the heating

demand of the building.

The investigations methods on various SAASHPs available in literature are briefly summarised in Table 3. It is apparent that basic DX-SAASHP and serial IX-SAASHP draw most attention. Experiments and theoretical analyses are two of the most common research methods. Simulation methods, especially using TRNSYS software, is mainly employed to study IX-SAASHP.

2.1. Direct expansion system

The DX-SAASHPs (see Figs. 2 and 3) use solar collectors as their evaporators to achieve higher *COP* due to higher evaporation temperature. Simulation results by Chow et al. showed a year-average *COP* of 6.46 [32]. Bare solar collectors (roll-bond evaporators) are preferably used in DX-SAASHPs to reduce the solar radiation loss by glass reflection

Table 1
Previous reviews on solar-assisted vapour-compression HP systems.

System	Reference	Contents
DX-	Kara et al., 2008 [5]	Review on DX-SAASHP
SAASHP		Mathematical model for exergy assessment
	Omojaro and Breitkopf, 2013 [6]	Review on DX-SAASHP
		Shortage of studies for SC
		Key components and important characteristics
		Common-used refrigerants
		Parameters for performance evaluation
	Amin and Hawlader, 2013 [7]	Review on DX-SAASHP for HW, drying and desalination in Singapore
	Facao and Carvalho, 2014 [8]	Review on DX-SAASHP
		Novel method to analyse DX-SAASHP for HW
	Shi et al., 2019 [9]	DX-SAASHP systems and the performance parameters
		Collectors in details
		Other components and refrigerants
		Optimal designs and control
		Review on simulation for collectors and the whole systems
		Applications in HW, SH, desalination and vaporisation of liquid fuels
CATTE	D 1 1 1 1 1 1 1 0 1 0	Future development trends Future development trends
SAHP	Ruschenburg and Herkel, 2013	 representation of SAHP: SAASHP, solar-assisted GSHP (SAGSHP), solar-assisted water source HP (SAWSHP), GSHP, ASHP,
	[10,11,12]	WSHP and photovoltaic/thermal (PV/T) systems
		Market-available systems in terms of companies, functions, configurations, heat sources, and solar collectors Analysis of market features.
	Oncomer and Hambacki 2007 [12]	Analyses of market factors Provious on groups and groups on SALIPs: SAASUP and SACSUP.
	Ozgener and Hepbasli, 2007 [13]	Review on energy and exergy analyses of SAHPs: SAASHP and SAGSHP Review on company models for SAHPs: SAASHP and CACSHP. Review on energy and exergy analyses of SAHPs: SAASHP and CACSHP. Review on energy and exergy analyses of SAHPs: SAASHP and SAGSHP. Review on energy and exergy analyses of SAHPs: SAASHP and SAGSHP. Review on energy and exergy analyses of SAHPs: SAASHP and SAGSHP. Review on energy and exergy analyses of SAHPs: SAASHP and SAGSHP. Review on energy and exergy analyses of SAHPs: SAASHP and SAGSHP. Review on energy and exergy analyses of SAHPs: SAASHP and SAGSHP. Review on energy and exergy analyses of SAHPs: SAASHP and SAGSHP. Review on energy and exergy analyses of SAHPs: SAASHP and SAGSHP. Review on energy and exergy analyses of SAHPs: SAASHP and SAGSHP. Review on energy and exergy analyses of SAHPs: SAASHP and SAGSHP. Review on energy and exercise the same and SAGSHP. Review on energy and exercise the same and SAGSHP. Review on energy and exercise the same and SAGSHP. Review on energy and exercise the same and SAGSHP. Review on energy and exercise the same and SAGSHP. Review on energy and exercise the same and SAGSHP. Review on energy and exercise the same and SAGSHP. Review on energy and exercise the same and SAGSHP. Review on energy and exercise the same and SAGSHP. Review on energy and exercise the same and SAGSHP. Review on energy and exercise the same and SAGSHP. Review on energy and exercise the same and SAGSHP. Review on energy and exercise the same and SAGSHP. Review on energy and exercise the same and SAGSHP. Review on energy and exercise the same and SAGSHP. Review on energy and exercise the same and SAGSHP. Review on energy and exercise the same and SAGSHP. Review on energy and exercise the same and SAGSHP. Review on energy and exercise the same and same an
	Haller et al., 2012 [14]	Review on component models for SAHP: SAASHP and SAGSHP Provious on CAASHP proteons in Canada
	Chu and Cruickshank, 2014 [15]	Review on SAASHP systems in Canada Parameters for performance cyclination.
		Parameters for performance evaluation Systems used in Consider residential content
	Kamel et al., 2015 [16]	 Systems used in Canadian residential sector PV/T technologies and HP systems
	Kainer et al., 2013 [10]	Economic analysis
		Applications of PV/T systems
	Buker and Riffat, 2016 [17]	Review on SAHP for HW: SAASHP, SAGSHP and PV/T
	buker and idnat, 2010 [17]	Key system components
		Common-used refrigerants
		Parameters to evaluate system performance and efficiency
	Wang et al., 2017 [18]	Review on SAHP for HW: SAASHP, SAGSHP and PV/T
	rrang et an, 2017 [10]	SAASHP system analyses in first and second laws
	Poppi et al., 2015 [19]	Review on SAHP for the domestic sector: SAASHP, GSHP, photovoltaic (PV) and PV/T
	roppi et an, 2010 [15]	Performance parameters at thermal energy, PV, building and economic levels
		Hydraulics and control
		Economic analysis
	Mohanraj et al., 2018 [20,21]	Review on SAHP: SAASHP, SAGSHP and PV/T
		Mathematical model for SAHP (energy and exergy analyses, artificial neural network modelling, transient system simulation
		life cycle assessment and control models)
		• Available innovations for performance enhancement (latent heat source, collector/evaporator, heat pipe, PV/T technologic
		inverter compressor)
		 Improvement in cycle design: two-stage compression cycle, cascade cycle, vapour ejector enhanced cycle, trans-critical cyc
		and organic Rankine cycle
		Common-used refrigerants
		Economic and environmental analyses
		Application of SAHP (drying, SH, and desalination) and limitations
	Wang et al., 2020 [22]	 Review on simulations (mainly using TRNSYS software) and experiments on SAHP (SAASHP, PV and PV/T)
		Performance parameters (at energy, economic and environmental levels)
		Economic and environmental analyses
		Comparison, limitation and future direction
	Sezen et al., 2021 [23]	Introduction on system configurations of SAHP (SAASHP and PV/T)
		 Analyses of the influence of ambient conditions (solar irradiance, air temperature, humidity and wind speed)

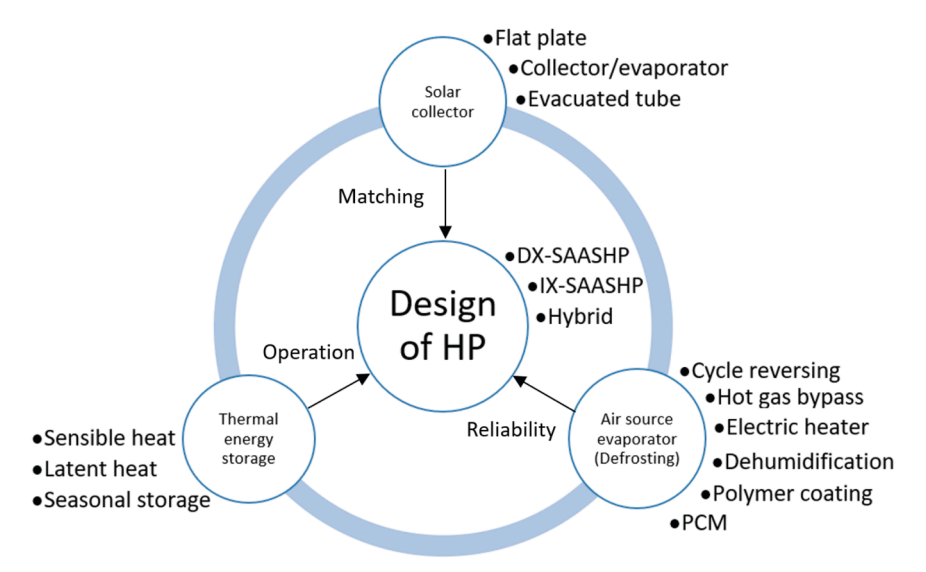


Fig. 1. Framework of this paper.

Table 2Categories of vapour-compression SAASHP.

DX-SAASHP	IX-SAASHP	Hybrid SAASHP
Basic	Serial	Basic
Dual-source	Dual-source	
Two-stage	Cascade	Cascade
Vapour ejector-enhanced	Composite	Trans-critical

and to extract thermal energy from ambient air.

Fig. 3 shows the ideal thermodynamic cycle on the *P-h* diagram of the DX-SAASHP system. The superheating at the inlet of the compressor and the subcooling at the outlet of the condenser are indicated. In the actual cycle, the flow resistance results in significant pressure drop at the outlets of the evaporator and the condenser.

Evaporator can be arranged in series or parallel to the solar collector in DX-SAASHPs. Fig. 4 shows a serial evaporator-collector system for HW [29]. This system has *COPs* ranging from 3.5 to 2.5 as water temperature increasing from 30 °C to 50 °C. Fig. 5 shows a parallel dual-source DX-SAASHP [34]. This system exhibits better *COP* than the DX-SAASHP shown in Fig. 3, especially at low solar irradiance [33,34,35]. The heat transfer rates in the solar collector and evaporator affect the distribution of refrigerant flows and hence determine the *COP*. Experimental results showed the *COP* of a DX-SAASHP in solar-source solely mode 30%–50% higher than that in ASHP mode [33]. Numerical simulation results showed that the averaged *COP* of a DX-SAASHP in dual-source mode is 14.1% higher than that in solar-source-only mode in low solar irradiance of 100 W/m² [34].

The DX-SAASHP of two-stage vapour-compression cycles has been developed for high temperature (60–90 °C) application (see Fig. 6) [36]. Fig. 7 shows the two-stage vapour-compression cycles on *T-s* diagram. The refrigerant evaporates in the solar collector to saturation state (8–1) and is compressed by the low-pressure compressor (1–2). The superheating vapour (2) is cooled in the flash tank by saturated liquid (7) up to saturated vapour (3). In the low-pressure cycle, the refrigerant is throttled in the expansion valve (7–8) and feed the evaporator in the 8 state. For the high-pressure cycle, the saturated vapour is compressed by the high-pressure compressor (3–4) and then condensed in the condenser (4–5), and finally expands at the expansion valve (5–6).

Kuang and Wang designed a multi-functional DX-SAASHP for SH, SC and HW provision, with a radiant floor, a fan and a water tank [37]. The experiment expresses a *COP* of 2.1–2.7 for SH-only mode. In SC-only mode, this system adopts a storage tank to balance the night cold

thermal energy storage and the daytime demand, but the cold energy storage efficiency (30%) and COP (2.9) are not satisfactory. In HW-only mode, the cycle provides 200–1000 L HW with a temperature of 50 °C daily. It should be noticed that this system is only studied in single-function modes. In multi-function mode, the interaction among components may result in heat losses and requires more energy input. The system in the multi-function mode needs to be further studied.

Vapour ejection can reduce pressure ratio of compressors and thus improve system efficiency. Zhu et al. proposed a dual-nozzle vapour-ejector to assist compressor and to reduce the energy consumption [38]. The arrangement of the vapour-ejector enhanced DX-SAASHP, as well as its *p-h* diagram and vapour ejector construction are shown in Fig. 8 (a), (b) and (c). The dual-nozzle vapour ejector connects the low-temperature (air source) and the high-temperature (solar source) evaporators. The simulation results of this system show that the *COP* and heating capacity are 4.6%–34% and 7.8%–52%, respectively, higher than those of the conventional vapour ejector-compression cycle. The ratio of pressures can be further reduced for a larger temperature difference between the two evaporators.

The vapour ejector enhanced DX-SAASHPs have been further developed in [39] and [40] (see Figs. 9-10). In [39], the superheated vapour discharged by the compressor condenses (2–3) and then flows into the throttle valve (3–4) and the liquid pump (3–6), respectively. The low-pressure stream absorbs heat from air source (4–5). The high-pressure stream evaporates to the superheated vapour in solar collector (6–7). The superheated vapour works as the primary flow of the vapour ejector and expands to a two-phase flow with little liquid (7-7') to entrain the vapour from the evaporator (5-5'). The two streams are mixed in the mixing chamber (8) and are then compressed in the diffuser (8–1) and the compressor (1–2). Theoretical analysis suggests that, compared with the conventional HP, this system can lead to increases by 15.3%, 38.1% and 52.8% in the *COP*, heating capacity and heating exergy output, respectively.

An adjustable DX-SAASHP system with a solenoid valve between the condenser and the vapour ejector was analysed theoretically [40]. It has a pure vapour ejector-compression mode and a pure solar-assisted vapour ejector-compression mode. The superheated refrigerant vapour condenses to saturated or subcooled states (2–3). In mode A, the liquid works as the primary flow of the vapour ejector directly. In mode B, the liquid evaporates (3–4) in solar collector and then works as the primary flow. The two-phase fluid is separated into saturated liquid (5–6) and saturated vapour (5–1) in the phase separator. The liquid part expands to two-phase fluid (6–7) and then evaporates to saturated or

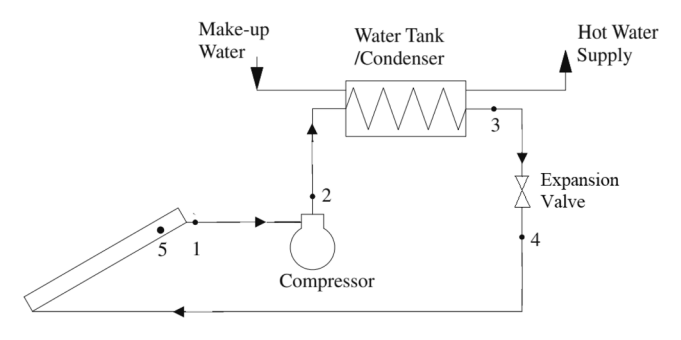


Fig. 2. Schematic of a DX-SAASHP (heating) (reproduced from [32]).

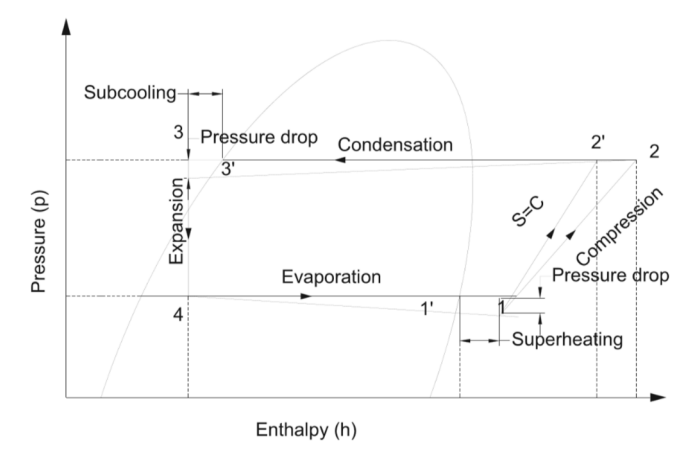


Fig. 3. P-h diagram of the DX-SAASHP [20].

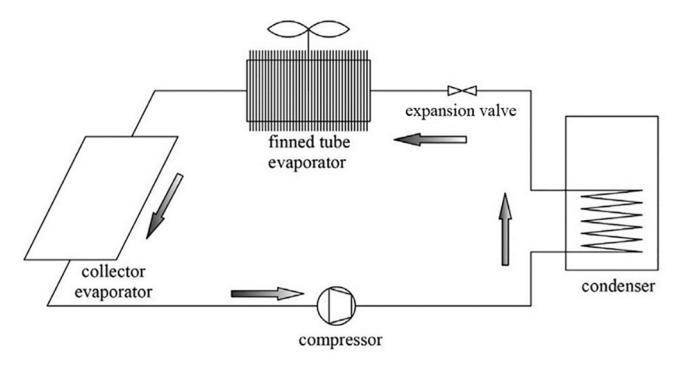


Fig. 4. Schematic of a DX-SAASHP for SC and HW (reproduced from [29]).

superheated states (7–8). This is the secondary flow of the vapour ejector. The vapour part is then compressed (1–2). The simulation results suggest that the *COP* and heating capacity are 13.8% and 20.4% higher than those of the conventional vapour-ejector enhanced vapour-compression HP. On average, this cycle outperforms the vapour-compression HP in *COP* by 25.1%. However, these concepts lack validations from practical experiments [45].

2.2. Indirect expansion system

IX-SAASHPs include serial and dual-source systems. In serial IX-SAASHPs, the thermal energy collected by the solar collector heats up the water in the water loop and the hot water is circulated to the evaporator of the HP. Dual-source IX-SAASHP enables both ambient air and solar energy as the heat sources. Generally, the systems of IX-SAASHPs are more complicated than DX-SAASHPs.

Serial IX-SAASHPs use the thermal energy collected by the solar

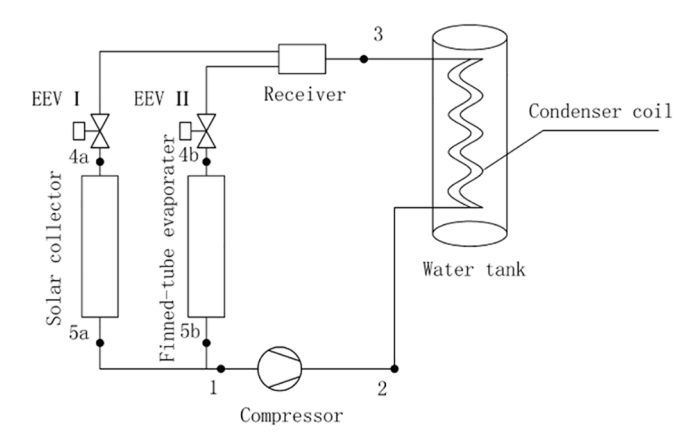


Fig. 5. Schematic of a parallel dual-source DX-SAASHP [34].

collector as the heat source. To balance the heat demand and supply. TES connects either to the solar collector and the evaporator (see Fig. 11 (a)) or to the condenser and the end use (see Fig. 11(b)). The TES also works as a buffer to reduce the noise and voltage shocks caused by the frequent start-up and shutdown of HP. In Fig. 11(a) SH by air is achieved by condensers placed in rooms. In Fig. 11(b) SH by water is achieved by circulating hot water to radiators. Although the utilisation of solar thermal energy increases the HP performance, the system COP is apparently lower than that of the HP due to the power consumed by the additional components. Experimental results of a serial IX-SAASHP showed the HP COP of 3.8 and its system COP of 2.9 [41]. Experimental results of a similar serial IX-SAASHP showed the HP COP ranging from 2.5 to 3.5, and the system COP is around 20% lower [42]. Fig. 12 illustrates a serial IX-SAASHP with dual TES tanks [43]. Compared with IX-SAASHPs in Fig. 11 (b), this system can reduce the frequency of HP start-up and shutdown.

Fig. 13 shows a dual-source IX-SAASHP which utilises both solar thermal energy and ambient air as the heat sources. Two evaporators are separately connected to an air—water heat exchanger and solar collector loop. A TES tank is in the solar collector loop. The HP provides HW and SH by air. Cai et al. conducted numerical and experimental studies of a multi-functional dual-source IX-SAASHP [44]. In HW mode, when the solar water temperature increases from 20 °C to 35 °C, the electricity consumption increases by 16.5% and the COP increases by 15.9%. The COP increases from 2.35 to 2.57 with the solar irradiance increasing from 0 to 800 W/m². In SH mode, when the solar water temperature increases from 20 °C to 40 °C, the COP increases by 20.2%, and the heating capacity increases by 42.6%. While the COP decrease by 26.3% and heating capacity decreases by 7.5% with the increase in indoor air temperature from 16 °C to 28 °C.

Numerical simulations were performed to compare the performance amongst the serial and dual-source IX-SAASHPs and hybrid SAASHP [46]. The results show that a hybrid SAASHP using a solar collector of $14\,\mathrm{m}^2$ achieves an SPF of 3.65 and consumes 2317 kWh electricity, while a serial IX-SAASHP using a solar collector of $30\,\mathrm{m}^2$ achieves an SPF of 3.53 and consumes 2401 kWh electricity. A dual-source IX-SAASHP using a solar collector of $14\,\mathrm{m}^2$ achieves an SPF of 3.70 and consumes 2289 kWh electricity. It is seen that the performance of the dual-source IX-SAASHP and hybrid SAASHP are almost the same. Due to the system simplicity the hybrid SAASHP is more attractive. However, some experimental studies draw opposite conclusions. Experimental studies in [47,48] show a COP of 4.0 of a serial IX-SAASHP and a COP of 3.0 of a hybrid SAASHP, respectively. Experiments in [49] found that a serial IX-SAASHP can reach a COP of 2.95, and a dual-source IX-SAASHP can reach a COP of 2.90.

Fig. 14 shows a novel component and system configuration proposed based on conventional IX-SAASHP [50]. The composite heat exchanger is used to replace the conventional water-to-water heat exchanger in

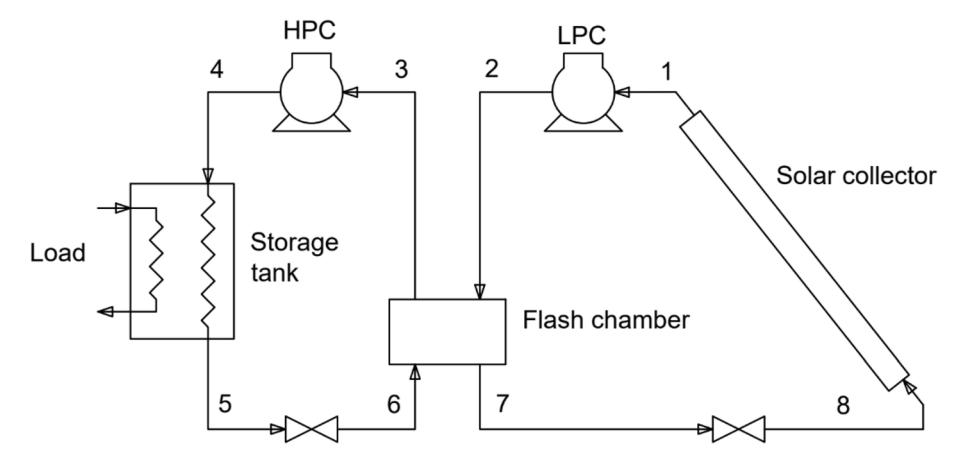


Fig. 6. DX-SAASHP with two-stage vapour-compression cycles (reproduced from [36]).

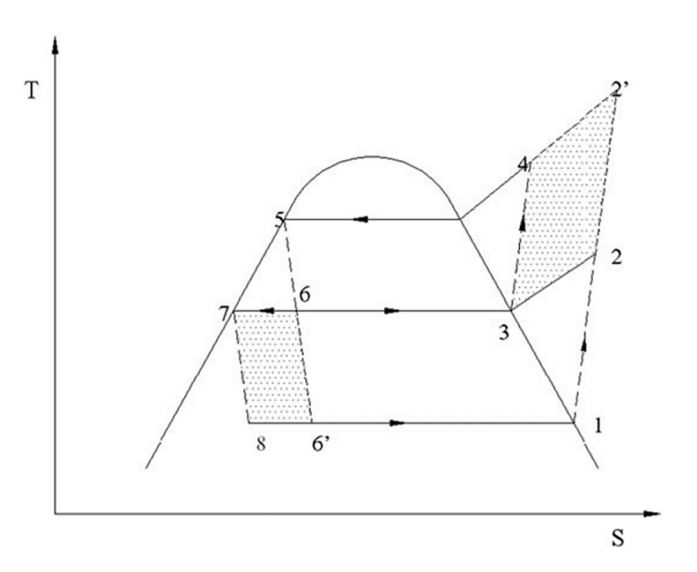


Fig. 7. T-s diagram of the two-stage DX-SAASHP [36].

serial IX-SAASHPs to absorb solar thermal energy and thermal energy from ambient air. A composite heat exchanger is designed by inserting a tube into a finned tube. Hot water from the solar loop flows inside the inner tube and refrigerant flows in annulus. This system has three working modes i.e. solar-only, air-only and dual-source modes. Experimental results show that, compared with the air-only mode, in the dual-source mode, the COP increases by 59% and the heating capacity increases by 62% at the ambient temperature of $-15\,^{\circ}$ C. When the temperature difference between solar water and ambient air is $5\,^{\circ}$ C, the COP and heating capacity in the dual-source mode are 49% and 51% higher than those in the air-only mode.

The use of two coupled compression cycles may incur high capital costs and electricity consumption. To reduce energy costs, a solar-assisted auto-cascade HP using a single compressor with zeotropic mixture R32/R290 has been proposed to maintain a wide range of outdoor air and heating circuit temperatures (see Fig. 15) [52]. To achieve an auto-cascade cycle, a phase separator is used with the cascade heat exchanger. The compressed superheated vapour (1–2) condenses to saturated or subcooled liquid (2–3). Then the liquid flows through the sub-cooler I (3–4) and expansion valve I (4–5) into the flash tank, where the two-phase fluid absorbs heat from the solar heating loop (5–6). The refrigerant is separated into the R290 dominant liquid (6–61) and the R32 dominant vapour (6-6v). The R290 dominant liquid is passed through expansion valve II (6v-7) to the cascade heat exchanger and vaporised completely (7–8). The R32 dominant vapour is transferred to the cascade heat exchanger (6v-9) and thoroughly condensed

via the sub-cooler II (9–10). Then the condensed fluid goes to the low-temperature evaporator through expansion valve III (10–11), absorbing heat from ambient air (11–12). Fluids from the low-temperature evaporator flow back through the sub-cooler II (12–13). Then it (13–14) is mixed with the vapour from cascade heat exchanger (8–14) and returned to the compressor through the sub-cooler (14–1). Simulation results suggest that, compared with conventional ASHP, this novel system increases *COP* and volumetric heating capacity by 4.2%–9.9% and 4.4%–9.7%, respectively. These improvements greatly rely on the heat absorption ratio and the composition of the zeotropic mixture.

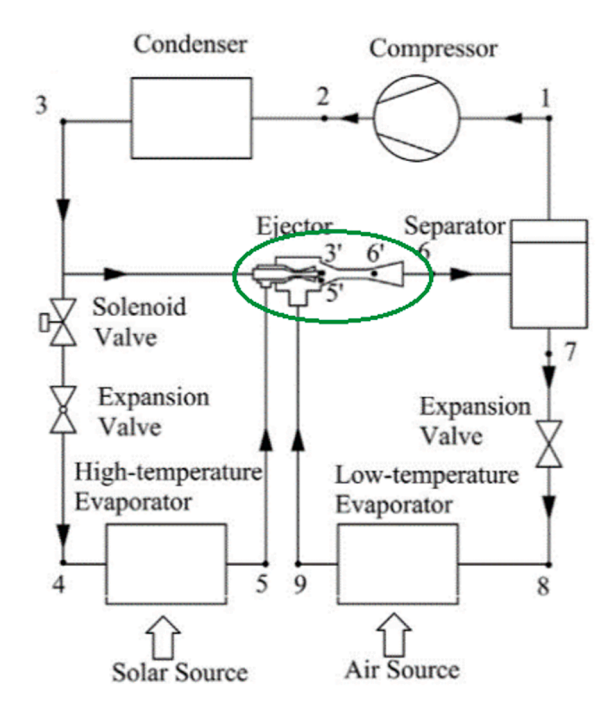
Fig. 16 illustrates a composite IX-SAASHP with an HP parallel to the solar collectors in the cold weather conditions in Canada [53,54]. The hot water leaving the solar collectors is further heated up in the condenser of the HP and then heat up the water in the TES tank. The HP absorbs residual thermal energy after the heat exchange and cools the water entering the solar collectors. The reduced collector inlet temperature improves the collector efficiency and thus the *COP*. It requires a lower capacity HP and consumes less electricity.

2.3. Hybrid system

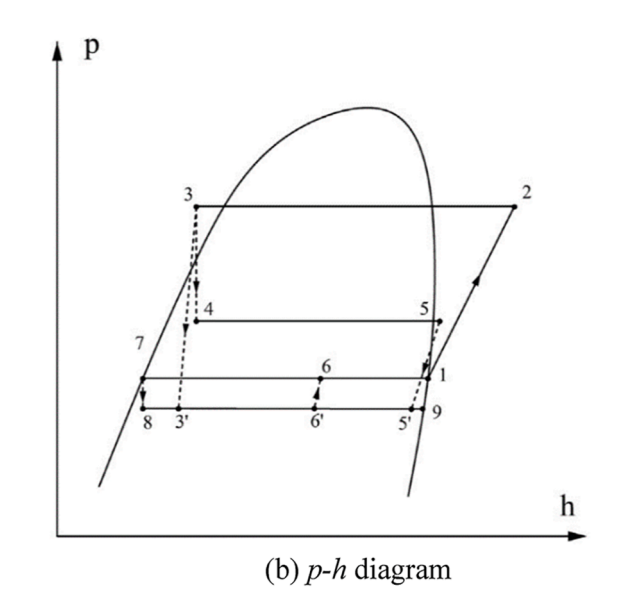
In hybrid SAASHPs (see Fig. 17), ASHP and solar collector water loop work independently. In Fig. 17(a) HW and SH by air is achieved by an ASHP and a solar heating with a TES tank. In summer, the ASHP can provide SC. In Fig. 17(b) an ASHP and a solar collector loop provide hot water to a TES tank to achieve SH by water. Compared with serial systems, the hybrid SAASHPs are more widely used [10].

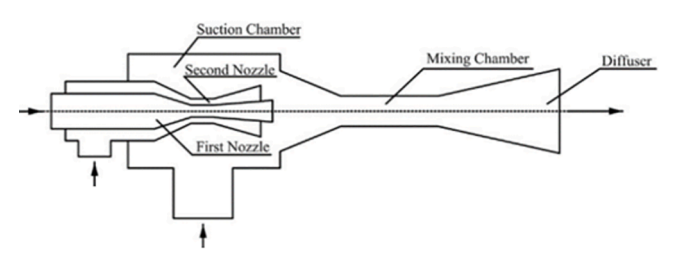
A single-stage vapour-compression HP cannot deliver heat above 50 °C at low ambient temperatures. To increase the temperature range between the outdoor air and the heating circuit, two-stage cascade HPs are used in the cold climate regions or to ensure the demand for a higher temperature lift. A solar-assisted two-stage cascade HP is proposed by Yerdesh et al. [51] where solar thermal collectors and a cascade ASHP simultaneously heat up the hot water in the TES tank (see Fig. 18). It was shown that combining a cascade ASHP with solar collectors increases energy efficiency by 30% compared with a conventional two-stage cascade HP. The cascade HP includes two single-stage cycles that operates separately with two different refrigerants, the low temperature cycle (LTC) and high temperature cycle (HTC). Using R32/R290 refrigerant pair, this system can have the maximum COP of 2.4 when the condensing temperature is 50 °C and evaporating temperature is -10 °C.

A solar thermal collector can be integrated in a hybrid trans-critical carbon dioxide (CO₂) HPs for SH, SC and HW (see Fig. 19) [55,56,57,58]. In SH and HW mode, the *COP* and heating capacity are about 2.3 and 6 kW [57,58], while in SC mode the *COP* and heating capacity are 4 and 8 kW, respectively [55].



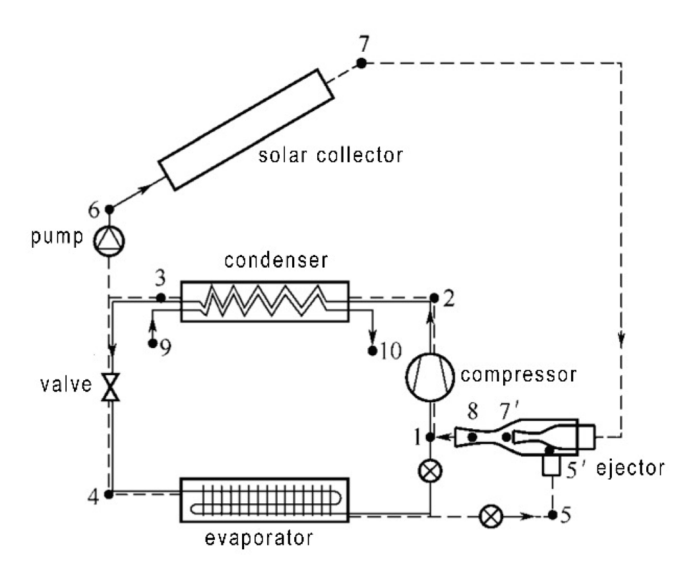
(a) Schematic of the system





(c) Dual-nozzle vapour ejector

Fig. 8. Dual-nozzle vapour ejector SAASHP system [38].



(a) Schematic of the system

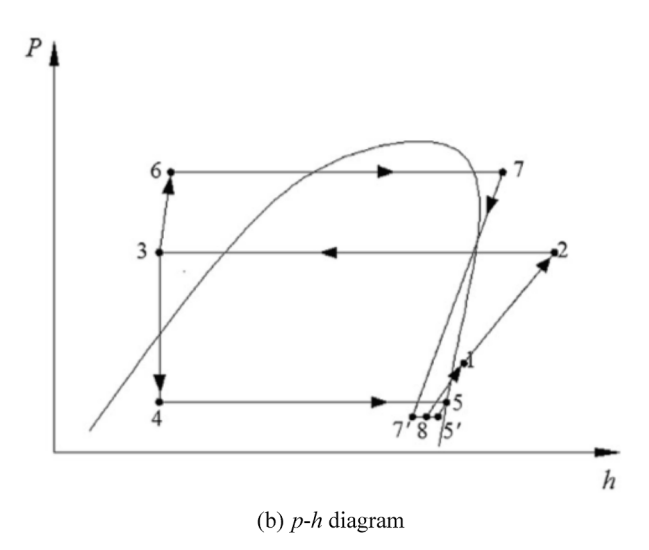


Fig. 9. Vapour ejector enhanced SAASHP system and the corresponding p-h diagram [39].

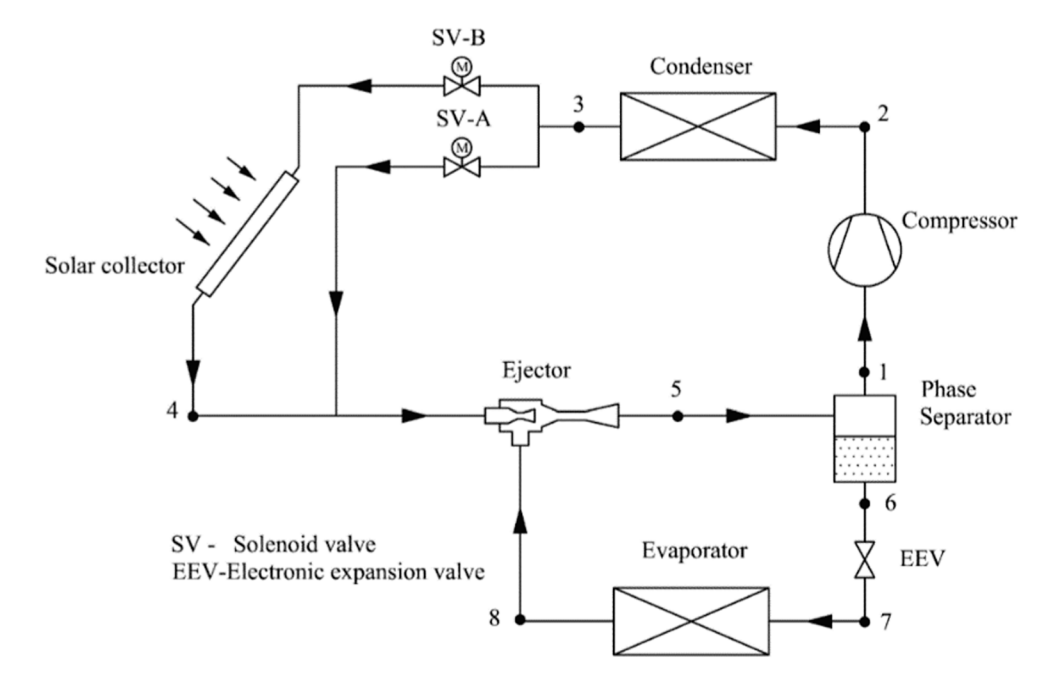
3. Solar collector

Solar collector is an important component for thermal energy input of SAASHPs. Flat plate collector is commonly selected in recent studies. To absorb more thermal energy from ambient air, the collector/evaporator is designed by coating solar selective materials on the surface of an evaporator. Collector/evaporator is mainly used in DX-SAASHPs. In IX-SAASHP, evacuated tube solar collectors draw more attention. Fig. 20 introduces the matching relation between solar collectors and system configurations. Table 4 lists some open literature where collector/evaporator and evacuated tube collector have been employed in SAASHPs. It can be noticed that systems using advanced solar collector can achieve a *COP* of 3–5. Especially, those for SH can work at ambient temperature below 0 °C.

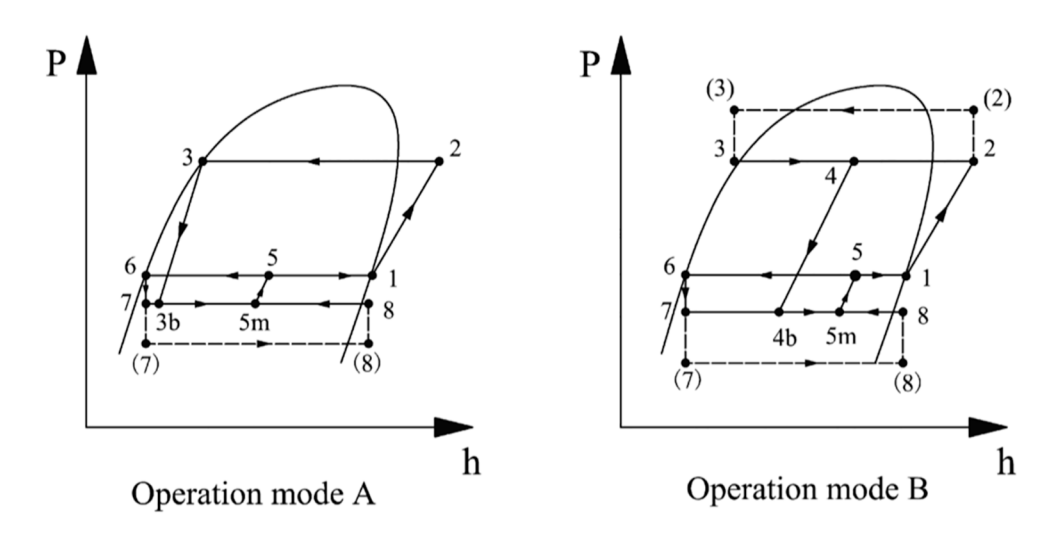
The thermal energy collected by a solar collector, $Q_{\rm sc}$, is determined by Eq. (5) [59]

$$Q_{\rm sc} = A\eta_{\rm sc} \{1 - a[(T_{\rm sc,in} - T_{\rm a})/L] + b[(T_{\rm sc,in} - T_{\rm a})/L]^2\}$$
 (5)

where A, $E_{\rm sc}$, and $\eta_{\rm sc}$ are the area, the average amount of energy received per square meter and collector efficiency, respectively, a and b are coefficients determined by experiments, $T_{\rm sc,in}$ is the water/refrigerant



(a) Schematic of the system.



(b) *p-h* diagram of two operation modes

Fig. 10. Adjustable vapour ejector enhanced SAASHP system [40].

temperature at the inlet of solar collector, T_a is the temperature of ambient air, and L is the average monthly value of atmosphere lucidity.

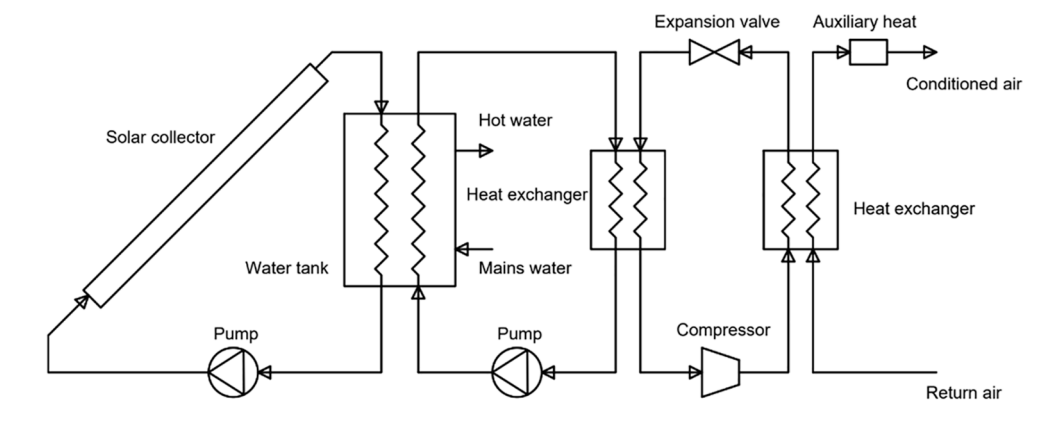
3.1. Flat plate solar collector

Flat plate collectors are commonly adopted in SAASHPs. Bare (uncovered) flat plate collectors enable to use thermal energy from solar radiation and ambient air. The experiment of Sun et al. [60] suggests that, at the outdoor temperature of 0– $10\,^{\circ}$ C, the collector efficiency of a bare solar collector ranges from 40% to 70%, where water vapour condensation occurs on the solar collector. The experiment study of Scarpa and Tagliafico [61] suggests that, due to water vapour condensation on the solar collector, a DX-SAASHP using a bare collector achieves a *COP* of 5.8 at weak solar radiation.

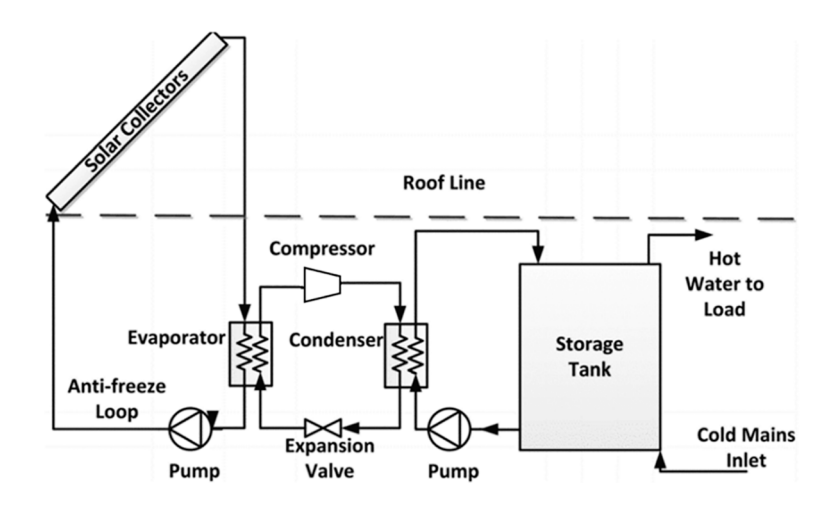
There is a noticeable influence of collector area on system

performance. Increasing collector area can enhance the SF of a SAASHP [30], almost in a linear relation [62]. Larger collector area can improve COP since it brings more solar energy input [63]. Both system configuration and collector area affect collector efficiency. With the same collector area of 30 m², the collector in a serial IX-SAASHP shows higher collector efficiency (62%–70%) than that in a hybrid SAASHP (with a η_{SC} of 54%–60%) [47,48]. With a smaller collector area of 20 m² in a serial IX-SAASHP, the collector efficiency ranges from 33% to 47% [41].

To improve collector efficiency, collector plate can be coated with black paintings [31,43,46,47,48,64,65,66,67,68,69]. Some collectors use serpentine tube or other special tubes between the plates [35,65,70]. The simulation results of a DX-SAASHP using an uncovered and coated collector with serpentine tube over a year showed daily *COP*s varying from 1.7 (in summer) to 2.5 (in autumn) with an average value higher than 2.0. [65]. The simulation results of a DX-SAASHP using a flat plate



(a) Space heating by air (reproduced from [63]).



(b) Space heating by water (reproduced from [15]).

Fig. 11. Serial IX-SAASHP.

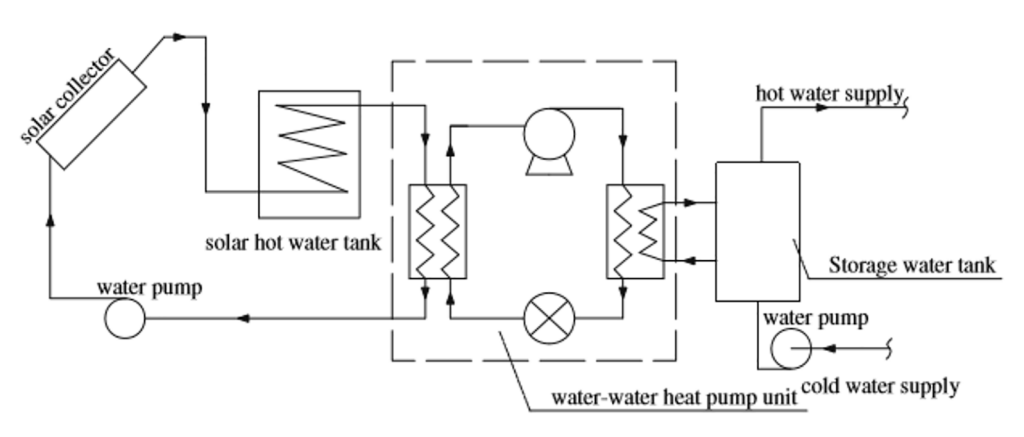


Fig. 12. Serial IX-SAASHP using dual water tanks [43].

collector with spiral tube showed monthly *COP*s between 4.0 (in summer) and 6.0 (in winter) [70]. The "contradictory" *COP*s in summer and winter are due to the high water temperature in summer which leads to high condensation temperature and low system efficiency. In terms of effect of weather conditions, the simulation results of a DX-SAASHP using a flat plate collector with serpentine tube showed *COP*s from 3.83 to 4.69 in sunny days [71]. Especially, in rainy winter, the average

COP can still achieve 3.3, with the lowest *COP* of 2.51. Similar conclusions can be drawn from experiments where the average *COP*s vary from 5.21 to 6.61 [72,73]. At a rainy night, *COP* can still reach 3.11 [74].

A novel flat plate collector is shown in Fig. 21 [67]. With an area of 11 m², this novel collector achieves an average collector efficiency of 67.2% at low operating temperature in a serial IX-SAASHP. The system *COP* is 2.19 and the *COP* of HP is 2.55. As a comparison, another serial

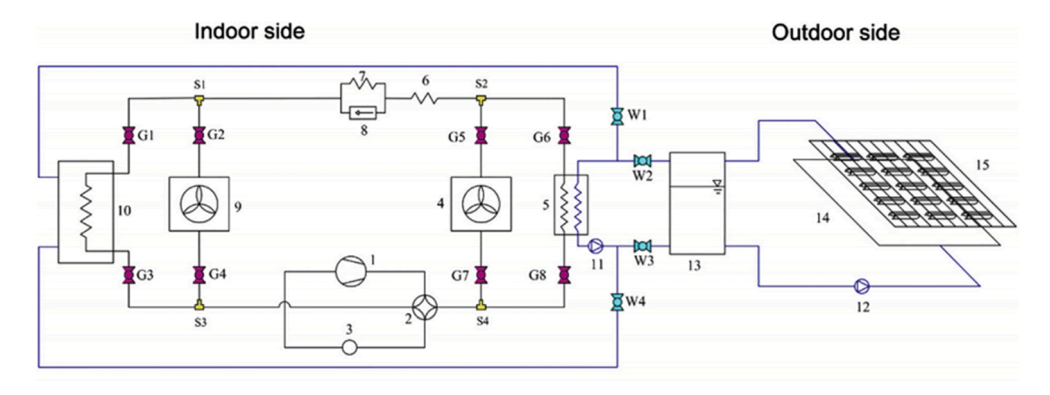
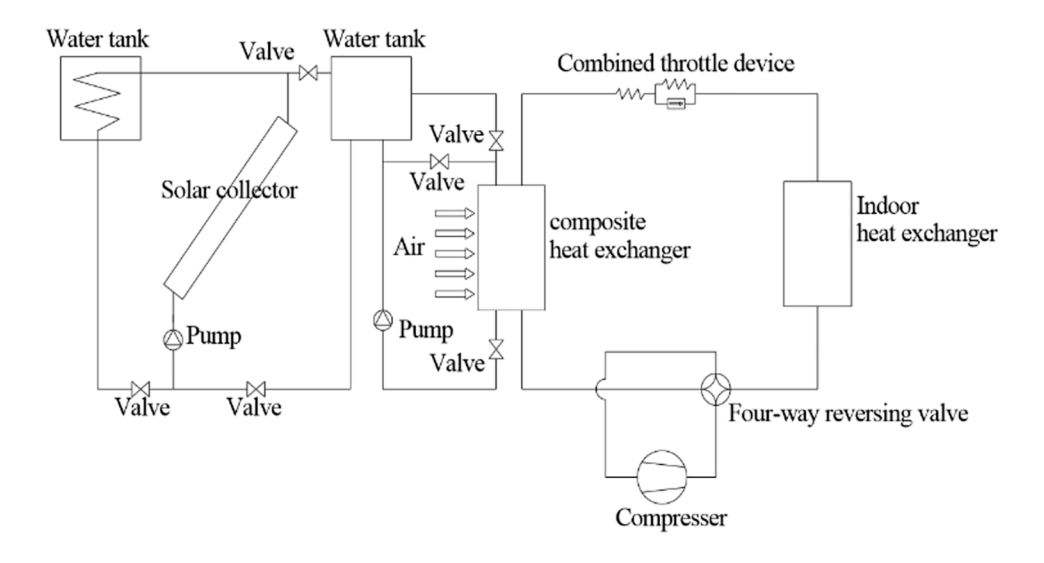
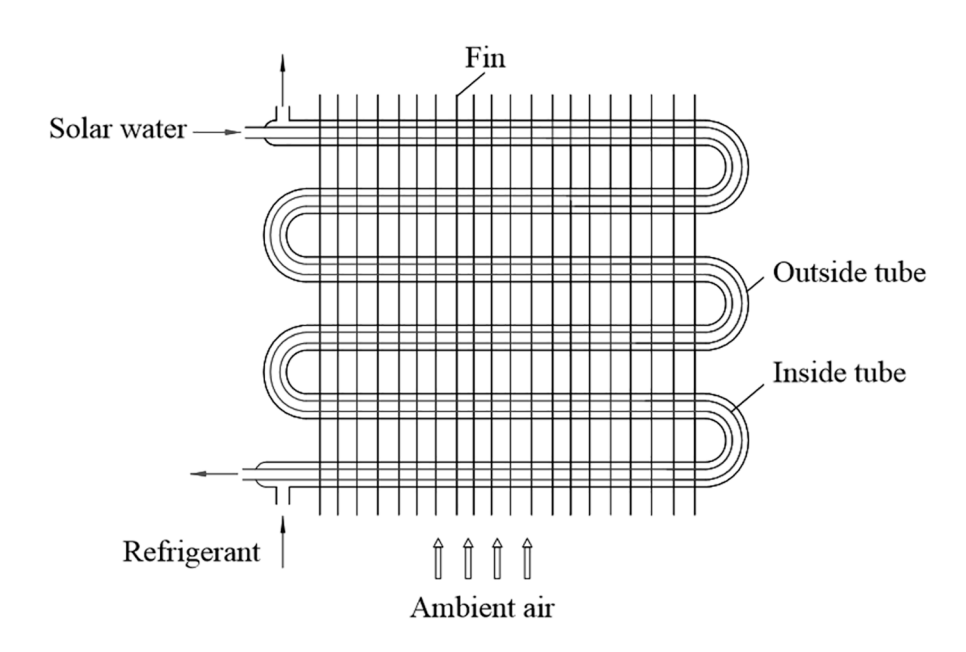


Fig. 13. Dual-source IX-SAASHP. 1 - compressor, 4 – air source evaporator, 5 – heat exchanger, 9 - condenser, 10 – water tank, 13 – water TES tank, 14 and 15 – two solar collectors. [44].

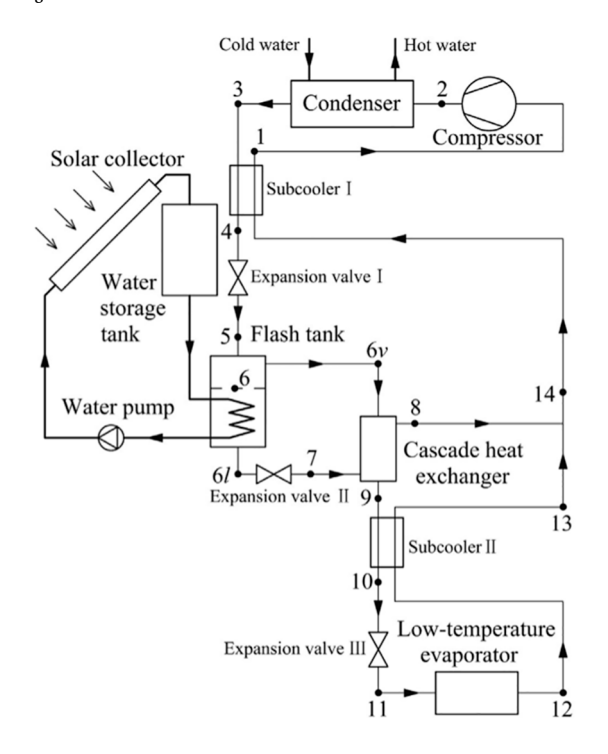


(a) Schematic of the system

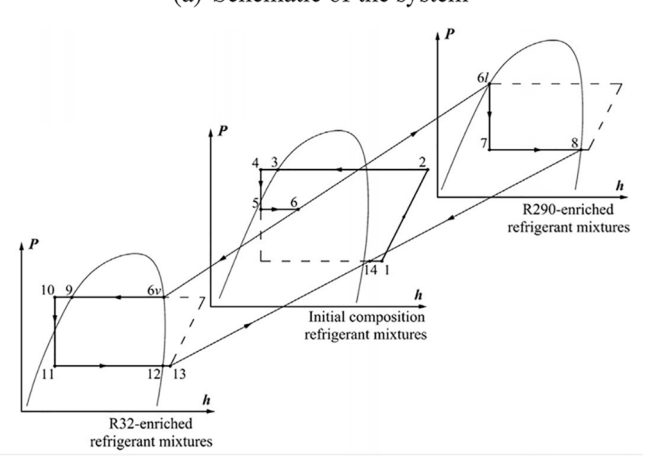


(b) Composite heat exchanger

Fig. 14. Dual-source IX-SAASHP with a composite heat exchanger [50].



(a) Schematic of the system



(b) *p-h* diagrams of the cycles

Fig. 15. Solar-assisted auto-cascade ASHP [52].

IX-SAASHP using a conventional flat plate collector obtains a collector efficiency of 60.1% but a system COP of 3.08 [75].

3.2. Solar collector/evaporator

The heating reliability of DX-SAASHP is better than that of direct solar heating, but still worse than that of ASHP. To further improve the reliability of DX-SAASHP, both solar and ambient thermal energies can be used by adding an air evaporator or using an uncovered flat plate collector. For example, a collector area of $3.24~\text{m}^2$ is considered ideal for an uncovered flat plate collector in a DX-SAASHP [76].

To earn higher year-average *COP*, a larger flat plate collector can be used but it is not economical [32]. Kaygusuz suggests that, when the number of collectors is doubled, *COP* is increased by 37% while the cost is increased by 65% [31]. Thus, to improve *COP* at low cost, collector/evaporator, designed by coating evaporator surface with solar selective materials, is a good alternative to extract more thermal energy. The

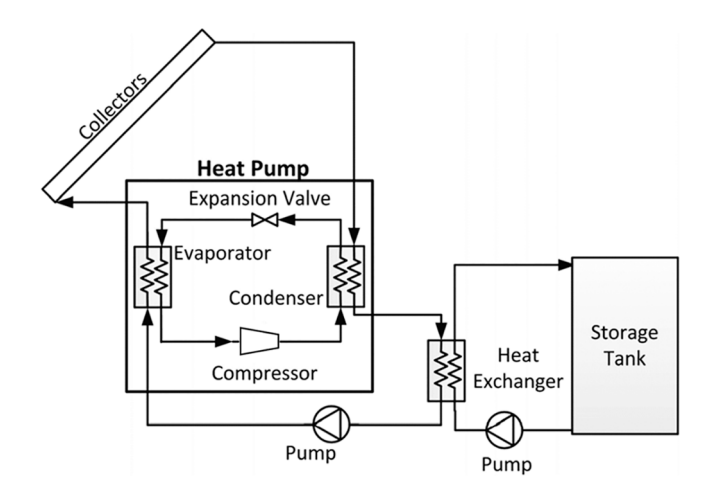


Fig. 16. A composite IX-SAASHP (reproduced from [15]).

average COP of a system using finned tube collector/evaporator is 2.94, increasing by 8.1% than that of conventional ASHP [77]. The average heating efficiency and exergy efficiency are raised by 20% and 8%, respectively.

3.3. Evacuated tube solar collector

IX-SAASHPs and hybrid SAASHP for SH require large collector area of flat plate collector. For a serial-hybrid SAASHP, a simulation study reveals a reasonable collector area of 35 m² for a covered flat plate collector [66]. To obtain a smaller system, the evacuated tube collector is an alternative. Simulation and experimental results of a serial IX-SAASHP using evacuated tubes show the maximum *COP*s of 6.33 and 6.38, respectively [78]. For a hybrid SAASHP using evacuated tube collectors, the *COP* can be around 5 at the highest daily solar irradiance [79]. The evacuated tube collector can be integrated with latent TES to further improve the thermal performance. For example, an experiment of a serial IX-SAASHP using both evacuated tube collector and latent TES shows a *COP* of 10.03 [80].

4. Thermal energy storage

TES is used to balance the energy demand and supply. It is essential for SAASHPs to mitigate solar energy discontinuity since an overcast for more than 20 min can lead to an apparent decrease in outlet temperature of the collector [83]. Both sensible and latent heat TESs are used in SAASHPs. The seasonal TES is suitable to regions with larger seasonal variations of solar energy availability and heating demand. Table 5 summarizes the studies involving latent heat and seasonal TESs. The studies on the sensible heat TES are summarized in Tables 6 and 7. On average, with optimisation in storage methods, systems can perform better with an *SPF* around 4–5.

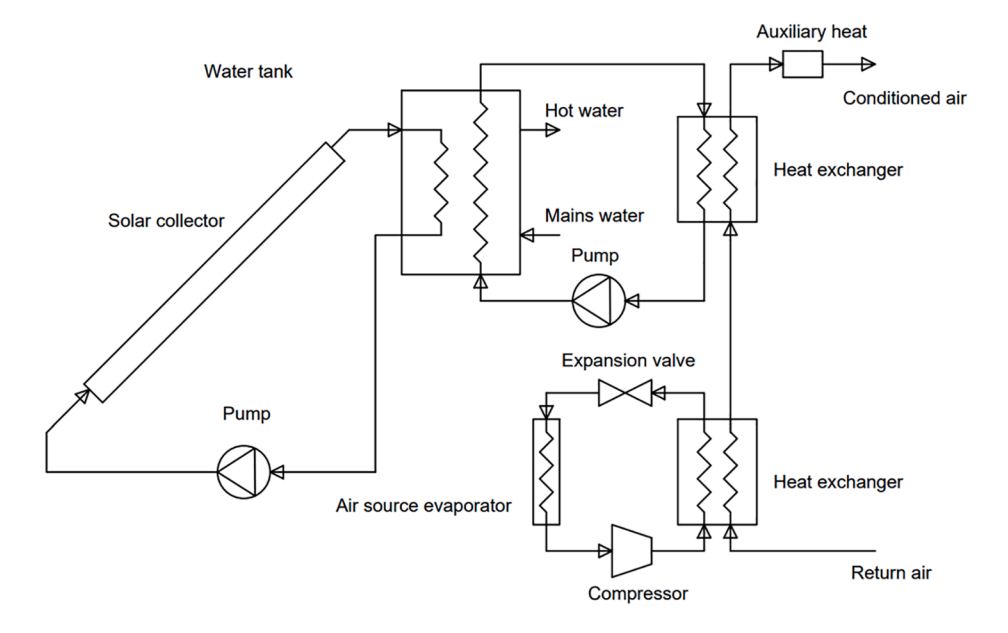
4.1. Sensible heat thermal energy storage

Typical air, geothermal and water source HPs make use of sensible heat as heat sources. The sensible heat can also be used to store thermal energy. Water and soil are widely used as the mediums for sensible heat TES. The maximum capacity for sensible heat TES, $Q_{\rm max}$, is determined by Eq. (6) [30]

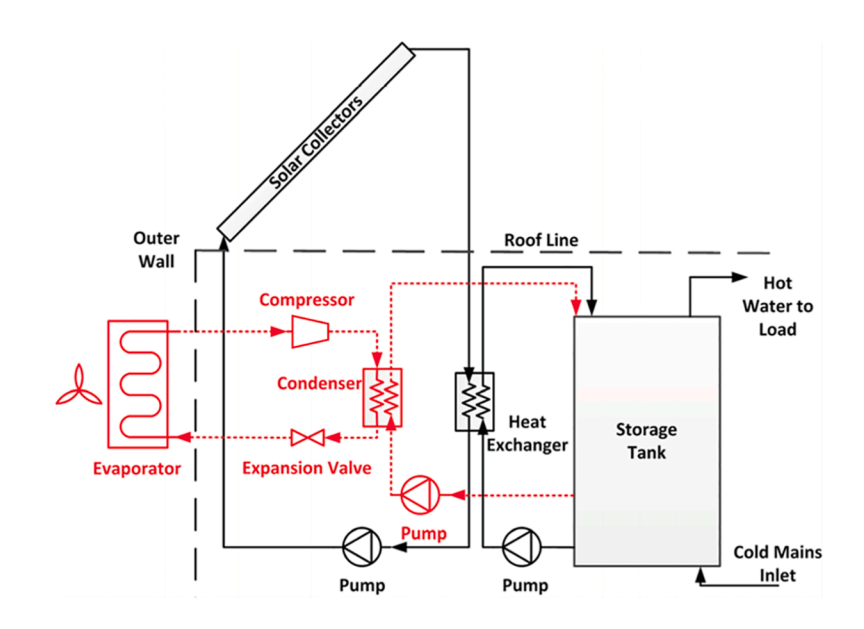
$$Q_{\text{max}} = \rho V_{\text{cp}} (T_{\text{max}} - T_{\text{min}}) \tag{6}$$

where ρ , V and $c_{\rm p}$ are the density, volume and specific heat capacity of the TES medium. $T_{\rm max}$ is the temperature of TES tank fully-charged and $T_{\rm min}$ the temperature of TES tank fully-discharged.

Geothermal TES can be integrated into a serial IX-SAHP using



(a) Hot water and space heating by air (reproduced from [63]).



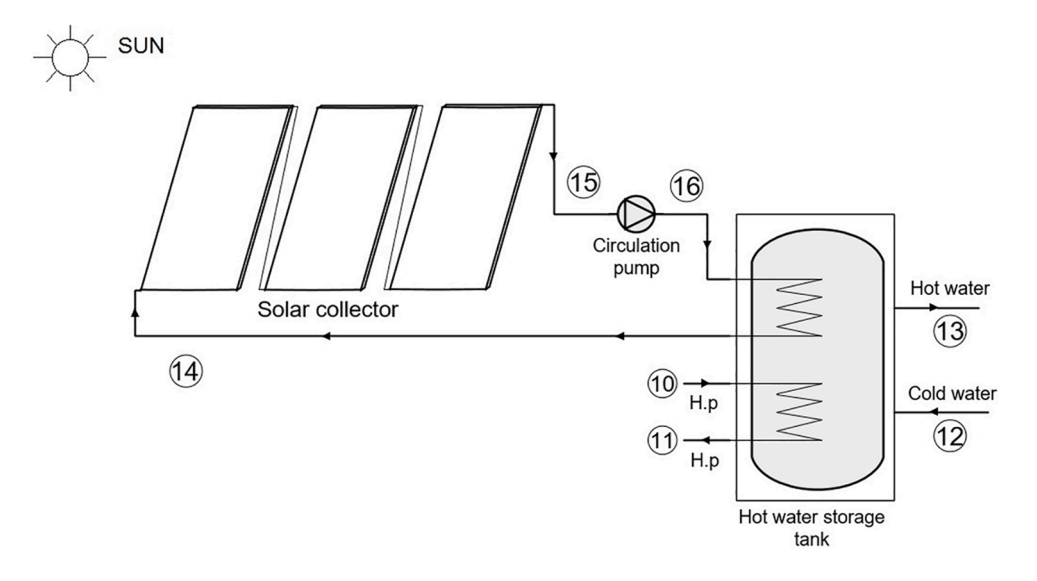
(b) Space heating by water (reproduced from [15]).

Fig. 17. Hybrid SAASHP.

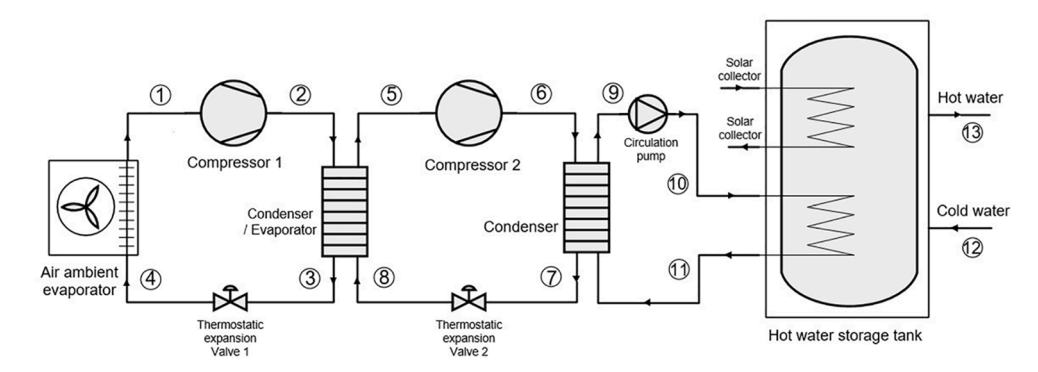
boreholes as the TES container (see Fig. 22) [84]. A numerical simulation of a solar-geothermal hybrid HP showed that the system can save energy by 2.08 TJ per year, equivalent to 70-ton standard coal and corresponding to 234-ton carbon dioxide emission [85]. An experiment demonstrated that the utilisation of ground TES helps to improve the *COP* from 2.95 to 3.36 compared with SAASHP [49]. However, since a deep borehole is required for sufficient heat exchange with ground, the excavation increases the installation cost of geothermal heat exchangers. Moreover, the heat stored in summer may not equal to the heat extracted in winter, influencing underground temperature balance [85].

Water TES is more popular than geothermal TES since water has higher thermal capacity and the manufacturing of water tanks requires much less capital cost. Water tank with high degree of thermal stratification shows 5.3% energy saving over one year than fully-mixed water

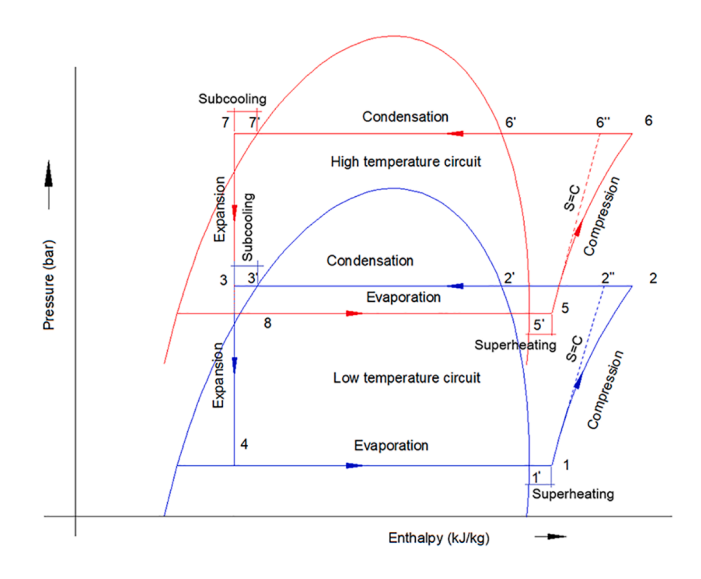
tank [86] because uniform distribution of water temperature reduces exergy [87]. Diffusers can be used to enhance thermal stratification. This increases energy efficiency of the system by 15%–20% compared with that using fully-mixed water tank [88]. Low water flow rate contributes to high degree of thermal stratification. Therefore, the water flow rate can be optimized considering the heating capacity and *COP* [44]. Water TES can be integrated with other components for heat recovery. An early study of a DX-SAASHP nested the evaporator/collector into a solar pond (TES) [89]. It achieved a *COP* higher than 3.0 in winter and the maximum *COP* of 8.4 in summer. A numerical simulation showed that recovering heat from waste-water stored can enhance the *SPF* of a SAASHP from 4% to 20% and recovering heat from drain water can improve the *SPF* by 2% [90].



(a) Solar collector loop



(b) Cascade HP loop



(c) *p-h* diagram.

Fig. 18. Solar-assisted cascade ASHP [51].

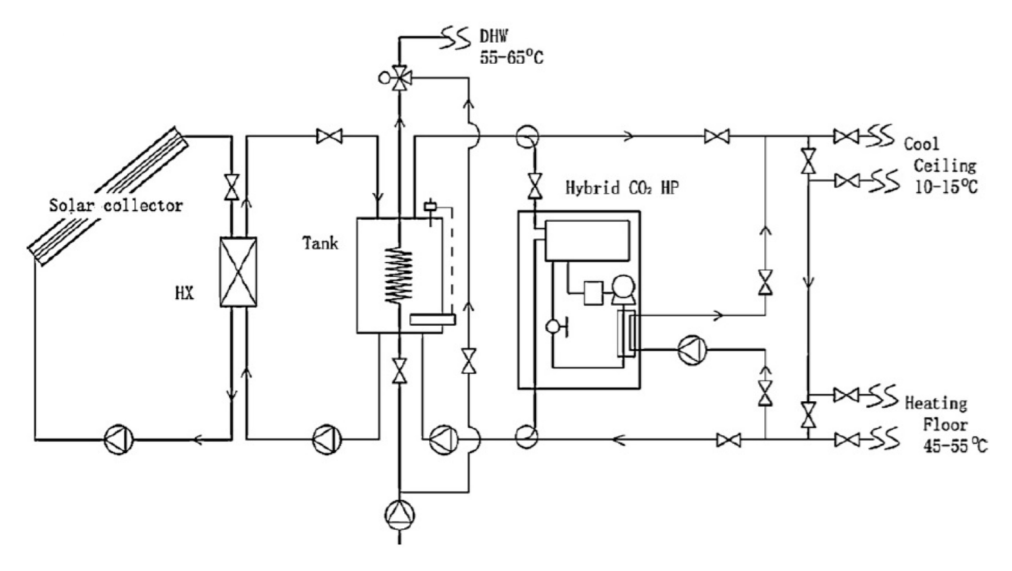


Fig. 19. Trans-critical SAASHP [55].

4.2. Latent heat thermal energy storage

Latent thermal energy is embodied in phase change material (PCM) at a constant temperature and is greatly larger than sensible thermal energy. A study on a serial/dual-source IX-SAASHP suggests that latent heat TES can increase the *COP* by 6.1% and 14% on sunny and cloudy days [81]. Another study designs a multi-function system which uses solar energy, latent TES and ground source [91]. In the latent TES mode, this SAHP achieves an average *COP* of 4.86, almost twice of that in the GSHP mode. When the latent heat TES is used as a heat source, a *COP* of 4.67 has been achieved.

PCMs are commonly stored in tanks and their storage efficiency is hardly influenced by system configurations. For example, for both serial IX-SAASHPs and hybrid system, the storage efficiencies of PCM-filled tanks are equal at 63% [47,48]. Due to some characteristics of PCM, such as the volume change during phase change process, tank selection for latent heat TES differs from that for sensible heat TES. Using a rectangular tank can decrease the melting time by 50% compared with using a cylindrical tank with the same volume and heat transfer area [92].

A novel triple-sleeve heat exchanger has been proposed as shown in Fig. 23 [93]. Refrigerant flows in the inner tube and PCM is filled between the inner and the middle tubes. Heat transfer fluid absorbs thermal energy in the solar collector and flows inside the outer tube. The effect of temperature of the heat transfer fluid on TES is higher than that of its flow rate. Ni et al. investigated a SAASHP with this triple-sleeve heat exchanger [94]. Compared with an ASHP, at an ambient temperature above 38 °C, cooling COP of the SAASHP using the novel heat exchanger is 17% higher; at an ambient temperature below -10 °C, heating COP of this system is enhanced by 65% [95].

Commonly used PCMs include paraffin, calcium chloride (CaCl₂), sodium sulphate (Na₂SO₄) and ice slurry. A novel serial/dual-source IX-SAASHP with paraffin for latent heat TES shows improvement in COP, especially on cloudy days [119]. A serial-hybrid SAASHP using CaCl₂ as the TES medium reaches a seasonal COP of 4.5 with a storage efficiency of 0.62 [96]. Generally, PCMs have poor thermal conductivity, which leads to higher thermal resistance and lower heat transfer. It also increases the time of charging and discharging processes, and thus impacts the overall system efficiency. However, studies involving both sensible and latent heat TESs suggest that the latent heat TES is superior to sensible heat TES. A dual-tank serial IX-SAASHP using Na₂SO₄ shows a COP of 10.03, about 3.5 times higher than that of a system only using sensible heat TES [80]. The collection efficiency (the ratio of thermal energy stored in water or PCM to the collected solar thermal energy)

increases by 50% when the latent heat TES is used, while the influence of the sensible heat TES is negligible. Another dual-tank serial IX-SAASHP using ice slurry as the PCM reaches an *SPF* of 4.6, where solar energy meets 78% of the heat demand [62].

Water/ice is the most available and eco-friendly PCM. Compared with an electrical resistance heating system, a serial IX-SAASHP using ice slurry as the PCM saves energy consumption by 86% [54,97]. However, a SAASHP using sensible heat TES can also save 81% of energy consumption. A model of a reversible ice storage tank, which uses three plate heat exchangers: two attached on the tank wall and one inserted in ice, was proposed and validated for solar heating [98,99]. Based on the model, the *SPF* of a SAASHP using ice storage is predicted to be around 5.0 [82]. For the ice storage buried in borehole, energy extraction can be influenced by ground properties [100]. Under two extreme ground conditions, energy injection of the two heat exchangers on the wall fluctuates by 6%, and the energy injection of the heat exchanger in ice significantly fluctuates by 20%.

It should be noticed that increasing collector area or latent heat TES volume can improve system performance. Taking economic factors into account, to achieve the same performance, increase in collector area is more beneficial [46,62,82].

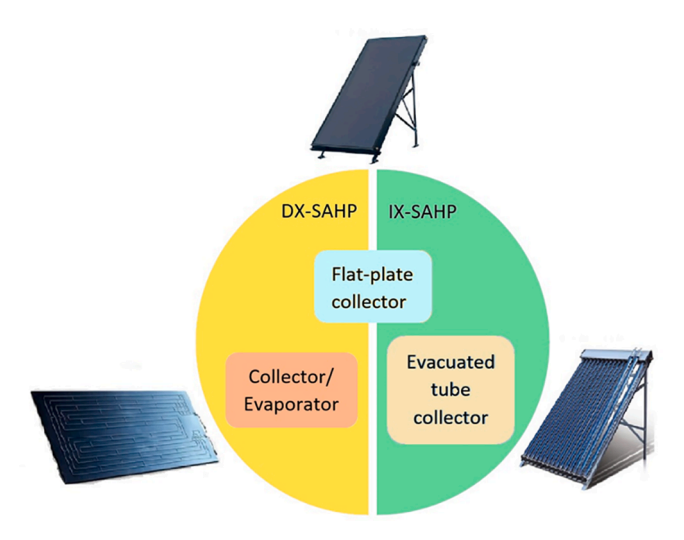


Fig. 20. Matching relation between solar collectors and system configurations.

 Table 4

 Utilisation of collector/evaporator and evacuated tube collector.

Authors	Location	Function	Refrigerant	Solar collector		TES		$T_{\rm a}$ (°C)	HC (kW)	COP	Comments	Related
		of HP		type	area (m²)	type	Vol. (m³)					work
Kuang et al., 2003	Qingdao, China 36°N	SH, HW	-	coated, covered	11	water	2.1	-10-4	4.99	2.19	-	
Huang et al.,2005 [35]	Taiwan, China 23°N	HW	R134a	bare, collector/ evaporator	1.98 sunny, 1.8 dark	water	0.24	34.9	-	3.32	-	
iang et al., 2011 [79]	-	SH	R22	evacuated tube	0 10 20 30	water	-	-1.2-9.5	10	3.3–4 3.3–4.3 3.3–4.6 3.3–5	-	
Caglar and Yamali, 2012 [78]	-	SH	R407C	evacuated tube	-	water	0.12	-	5.87	5.56	_	
Deng et al., 2013 [57]	Shanghai, China 31.17°N	HW, SH	CO_2	evacuated tube with compound parabolic concentrator	30	water	0.5	-5-5	-	2.38	A trans-critical hybrid SAASHP	[55,58]
He et al., 2014 [177]	-	HW	R134a, R600a, R22	covered, heat pipe	-	water	-	10–30	-	3.69–5.27	_	
Chaturvedi et al., 2014 [153]	-	HW	R134a	collector/ evaporator	3	-	-	-	0.366-0.603	1.7–5.61	-	
He et al., 2015 [170]	London, UK 51°N	HW	R134a	covered, heat pipe	2.4	water	0.03, 0.2	25	2.253	4.93	_	
Vang et al., 2015	-	SC, SH, HW	R407C	evacuated tube	-	water	0.15	7, 12, 20	2.56-4.24 (SH)	3.75-4.72 (SH)	_	[172]
Shan et al., 2016 [181]	Beijing, China 40°N	SH	-	evacuated tube	-	water	0.72, 0.8	-13.3-4.5	3.9	2.5–3.0	-	
Dong et al., 2017 [77]	Taiyuan, China 38°N	SH	R407C	coated, collector/ evaporator	0.4	Na ₂ SO ₄	0.8	-15-7	0.186	2.94	-	
Youssef et al., 2017 [81]	London, UK 51°N	HW	R134a	evacuated tube	3.021	water paraffin	0.3 30 kg	-	0.54-0.81	4.21–4.99	A serial/dual-source IX-SAASHP	
Buker and Riffat, 2017 [204]	-	SH, HW	R134a	solar thermal roof	1.92	water	0.055	27	_	2.29		
Liu et al., 2017 [206]	-	HW	-	evacuated tube	-	water	-	-5 7	42–55 53–65	1.8–2.7 2.6–3.2	Using a composite heat exchanger	
Youssef et al., 2017 [244]	London, UK 51.5 °N	HW	-	evacuated tube	3.021	water PCM	0.3 30 kg	-	9.632	4.7		
Li et al., 2018 [235]	-	SH	R134a, R1234yf, R141b	evacuated tube	33	water	-	20	20.9	4.2	An ejector enhanced DX-SAASHP	
Lee et al., 2018 [236]	Seoul Korea, 37 °N	HW	R1233zd(E), R134a	air-based flexible solar collector	35.2	water	0.6	2.08–10.92	0.83-3.29	1.12–3.99		
Kim et al., 2018 [209]	-	HW	R134a	collector/evaporator	24	water	-	21	7.21	3.4		
Han et al., 2018 [239]	-	SH, HW	-	evacuated tube	10	PCM water	510 kg 1	-23.4-20	0–45	0–8.3		
Huan et al., 2019 [205]	Xi'an, China 34 °N	HW	-	evacuated tube	860	water	55	24–37	2.8x10 ⁶ - 3.2x10 ⁶	4.87	Serial IX-SAASHP	
Aktas et al., 2019	_	HW	R410A	double pass collector	860 -	– Paraffin	- -	_	2.7x10 ⁶	10–20 3.3–3.8	Hybrid SAASHP	
[223] Stritih et al., 2019	_	SH	R407C	evacuated tube	25	RT42 paraffin	_	_	_	4.3–5.7		
[225]						RT 31 water	3					

Table 4 (continued)												
Authors	Location	Function	Refrigerant	Solar collector		TES		$T_{\rm a}$ ($^{ m o}$ C)	HC (kW)	COP	Comments	Related
		of HP		type	area (m²)	type	Vol. (m³)					work
Kong et al., 2020 [195]	Qingdao, China 36 °N	HW	R134a	microchannel solar collector	2.09	water	0.2	-3.4-10.7	0.6–1.1	1.65–3.43	A DX-SAASHP using microchannel condenser	[197]
			R290					-3-14.8	0.5-1.4	1.26-4.61		
Xian et al., 2020 [201]	Guangzhou, China, 23 °N	HW	R134a	PCM microchannel solar regenerator	1.11	water	0.04	8–15	0.35-0.55	1–4		[202]
Kutlu et al., 2020 [203]	I	HW	R134a	evacuated tube	4	PCM	0.15	9–25	1	3.4-4.6		
Ran et al., 2020 [207]	I	SH	R410a	flat plate collector with fan	7	I	ı	7	0.58-0.82	3.12–3.89		
Vega and Cuevas, 2020 [241]	ı	SH	ı	evacuated tube uncovered	22.5 22.5	water	0.3	10.2	ı	SPF 3.8–4.7 SPF 3.7–3.8		
		HW	ı	evacuated tube uncovered	225 225	water	22.7	10.2	ı	SPF 3.3–4 SPF 2.8–2.9		
Liu et al., 2020 [208]	Xining, China 36.6 °N	SH	ı	evacuated tube	10	water	8.0	-18.2 - 29.88	ı	2.3-4.2		[247]
Ji et al., 2020 [217]	1	SH	1	collector/evaporator	1	ı	1	5-15	1.3-1.8	2.2–2.6		
Li et al., 2020 [222]	Suqian, China 34 °N	SH, HW	R134a	air-type PCM evacuated tube	16	water	0.2	-3.1-11.9	2.6–3.6	2.5–6.5		
Treichel and Cruickshank, 2021 [219]	1	HW	R134a	air-type solar collector	1.26	water	0.189	1	I	1.9–2.4		[220,221]

4.3. Seasonal thermal energy storage

Solar TES includes daily and seasonal storages. The daily storage stores solar thermal energy collected during daytime and releases it at night. The seasonal TES stores the solar thermal energy collected in summer for heating in winter and/or in winter for cooling in summer. The seasonal TES is suitable to high latitude regions where seasonal solar energy and heating demand are dramatically mismatched [101]. Seasonal TES allows solar energy to provide more than 50% of the annual heating demand [102]. Compared with daily TES, seasonal TES requires large storage volume and collector area, consequently high cost [30].

Commonly used mediums for seasonal TES include water, gravelwater, ground and aquifer. Different mediums require different startup time to pre-heat surrounding soil up to normal operating conditions [102]. Tanks using water and gravel-water need to be buried (partly) into the ground. The ground and aquifer are directly employed as underground TES mediums. The buried water tank can be independent to ground properties due to its good insulation [102]. This additional insulation cost can be partly compensated by lower excavation cost. The results of a serial IX-SAASHP using an underground hemispherical surface tank for seasonal TES suggest that a small burial depth is capable of achieving desired annual COP and temperature of the storage tank [68,69]. The aquifer and ground TESs have better economic efficiencies than burial tanks [103]. Combining cost effective methods with high thermal capacity methods may optimise the system performance. For example, a system combining hot water and ground storages achieves an SF of 74% and a system COP of 4.4 [104]. It is worth noting that the change in ground temperature may bring disadvantages to environment [30].

Water has higher specific heat capacity while solid mediums allow higher temperature range for higher TES capacity [105]. In the cold climate regions, since the heat loss increases with the increase in temperature difference between storage mediums and surroundings, low-temperature seasonal TES is suitable [106] and benefits for storage stratification and thus storage efficiency [107]. Lower temperature of the fluid entering solar collector also improves collector efficiency [108]. PCM is a promising medium for low-temperature seasonal TES. The size of the latent heat TES is much smaller than that of a sensible heat TES. Numerical simulations were conducted to examine the annual periodic performance of a dual-source IX-SAASHP using a seasonal latent heat TES [109]. This system achieves an SPF of about 4.2.

5. Defrosting

Frosting is an issue influencing the reliable operation and efficiency of ASHPs in winter, especially in humid regions. Frost build-up on the surface of evaporator deteriorates heat transfer and efficiency and eventually shutdown of ASHPs [110,111]. The mechanisms of frosting and defrosting on the surface of evaporator are reviewed in [112,113,114]. Song et al. [114] comprehensively reviewed the defrosting methods including cycle reversing [115], hot gas bypass [116], electric heater [117], dehumidification [118] and polymer coatings [119]. The principle of the cycle reversing, hot gas bypass and electric heater is to melt the frost layer. The periodic defrosting required not only consumes electricity but also causes mismatching to the heating demand. The cycle reversing requires a well-designed control strategy to balance the SH demand and effective defrosting [115]. The dehumidification requires replacing or regenerating desiccant periodically as the moisture absorption capacity drops [118]. The polymer coating enables the reduction of the surface free energy and ice adherence force and hence delays frosting [119], where the challenge is to sustain the performance of the coating surface.

TES can assist the conventional defrosting methods [114,120]. As shown in Fig. 24, a PCM storage is parallel to the condenser [121]. During the period of reverse-cycle defrosting, no thermal energy is

Fig. 21. A novel flat plate collector [67].

provided for indoor SH. The stored heat assists to shorten the defrosting period by 38% [122]. The PCM storage is placed around the compressor to use the waste heat [123]. During the reverse-cycle defrosting, ASHP continues to provide SH because the stored waste heat is delivered to both indoor and outdoor heat exchangers. The defrosting time and total energy consumption is 65% and 27.9%, respectively, lower than conventional reverse-cycle defrosting. Over the whole test period, the *COP* and total heating capacity increase by 1.4% and 14.2% with the power input increasing 12.6%.

Fig. 25 shows an ASHP using a PCM-filled tank and an additional evaporator coated with desiccant in series [124]. This system enables continuous heat provision in both heating and regeneration modes. In the heating mode, air is dehumidified as it flows through the desiccantcoated evaporator (9) and then flows through the evaporator (12). Refrigerant is condensed in a condenser embedded in water TES tank (4) and then releases the residual thermal energy in the PCM TES tank (6). Refrigerant absorbs the latent heat released during air dehumidifying process in the desiccant-coated evaporator (9). This increases evaporation temperature of the evaporator (12) to avoid frosting. In the regeneration mode, refrigerant is condensed in a condenser embedded in water TES tank (4) and releases the residual thermal energy for desiccant regeneration as it flows in two evaporators (9 and 12). The refrigerant vaporises as it flows through the PCM TES tank (6) and absorbs the stored thermal energy. Experimental results of this ASHP shows a COP of 2.81, 7.3% and 46.3% higher than those of hot-gas bypass defrosting and electric heater [124]. Heating performance of ASHP is also superior to that of ASHP using reverse-cycle defrosting, especially in the cold weather conditions [125].

For SAASHP, defrosting is only a concern for outdoor evaporators. Solar thermal energy helps to reduce frost on solar collector [126]. Kong et al. [127] numerically and experimentally studied a DX-SAASHP under frosting conditions. The results showed that frosting on solar collector can be significantly delayed. Experiments [128] show that the frosting on a solar collector is much slower than that on an evaporator and after a 6-hour experiment, frost is merely seen on the solar collector. At a lower solar irradiance of 100 W/m^2 and a higher relative humidity of 70%, no frost is observed when the ambient temperature is higher than -3 °C.

6. Observations and outlook

Current studies on SAASHP focus on the match and optimisation of system configuration. However, there is a lack on the optimisation of each component and its matching application in SAASHP. This section summarises recent research status in terms of system configuration, solar collector, TES, working conditions, refrigerants and their influences on system performance. In addition to Table 4 summarizing the details regarding the utilisation of collector/evaporator and evacuated tube solar collector and Table 5 summarizing the details about the studies of SAASHPs using latent heat and seasonal TESs, Tables 6 and 7 give the details of the typical studies of DX-SAASHP and IX-SAASHP and Table 8 gives the details of some advanced SAASHP configurations. The statistic summaries given in these tables provide an overall view of the studies on this topic and sufficient information for further analysis below.

Working fluid determines the selection of compressor and therefore

the corresponding components. Fig. 26 summarises the number of open literature per year for SAASHPs using different refrigerants. It can be seen that, generally, the number of studies on SAASHPs shows an apparent increase in the past 10 years. Currently, refrigerants such as R22, R134a, R32, R410A and R407C are normally used in HPs due to their good thermodynamic and thermophysical properties [20]. Due to the composition shift and temperature glide, the currently used mixed refrigerants have technical limitations [129]. The parameters that determine the environmental impacts of refrigerants are the ozone depletion potential (ODP) and global warming potential (GWP). These parameters are high for the specified refrigerants. International environmental protocols [130,131,132] have imposed restrictions on the use of refrigerants according to ODP and GWP parameters. According to the Kigali Agreement [131], natural refrigerants such as hydrocarbon refrigerants and carbon dioxide (R744) were found to be long-term sustainable options for HPs [20]. For example, the performances of R1270 and R290 are closer to that of R22 but their flammability requires more safety considerations while retrofitting [83]. Current studies on environment-friendly refrigerants with low GWP, such as R32 and R290, are insufficient and need to be further investigated. R32 is a more environment-friendly alternative refrigerant to R410A in HPs and it is most commonly used in Japan for supplying HW. However, due to flammability (A2L) issues some countries are researching other retrofits, such as R454B. R290 is the most popular refrigerant for HPs in Europe not only for HW but also for SH applications. Recent increase in refrigerant inventory limit (IEC 60335-2-89 [133]) enables greener refrigerants such as R32 and R290 in these applications.

The geographic location affects solar availability and thus the research interests on SAASHP. Fig. 27 shows the number of investigations on SAASHPs in different countries. It can be noticed that the majority of studies have been located in China (48%), Turkey (10%), the US and Canada (5%). The studies in the UK is only 3%. SAASHPs for the domestic sector are mainly investigated by researchers from midlatitude (20° - 50°) countries where SH is required in winter and HW is required throughout the year under the medium solar energy availability and temperate climate conditions (-15 °C - 30 °C). SAASHPs for high-latitude areas need to be further investigated.

Generally, the higher solar irradiance leads to the higher COP of SAASHP [33,71,73,77,134,135,136,192]. For example, a numerical simulation of DX-SAASHP for HW has tested the effects of various parameters (see Figs. 28 and 29) [73]. As solar irradiance increases from 300 to 1000 W/m², COP increases from 4.2 to 6. In this process, solar collector efficiency decreases from 1.5 to 0.85. It should be noticed that an uncovered collector is used in the study which absorbs thermal energy from both solar irradiation and ambient air. At lower solar irradiance, the collector mainly absorbs thermal energy from ambient air and achieves an efficiency over 1; at higher solar irradiance, the collector mainly absorbs thermal energy from solar energy and the efficiency is lower than 1 because of heat loss. For a covered collector, the trend is the same but less apparent [108].

In terms of ambient temperature, as Fig. 29 shows, high ambient temperature leads to higher *COP* and collector efficiency [73]. With the increase of ambient temperature from 5 °C to 35 °C, *COP* increases from 4.5 to 5.7, and collector efficiency increases from 0.75 to 1.07 since as ambient temperature increases, collector can earn more thermal energy

Table 5Studies of SAASHPs using latent heat and seasonal TESs.

Authors	Location	Function	Refrigerant	Solar collector		TES		T_a (°C)	$T_{\rm con}$	HC (kW)	COP	SPF	Comments	Related work
		of HP		type	area (m²)	type	volume (m³)		(°C)					
Esen, 2000 [101]	Trabzon, Turkey 41°N	SH	-	flat plate	30	CaCl ₂	1090 kg	4.5–16.4	-	_	_		-	
Kaygusuz, 2000 [47]	Trabzon, Turkey 41°N	SH	R22	coated, flat plate	30	CaCl ₂	1500 kg	-3-16	40–55	0.04	4 for serial, 3 for hybrid systems		A serial-hybrid SAASHP	[31,48,64,66,96,224]
Yumrutas et al., 2003 [69]	Isparta, Turkey 37.8°N	SH	-	coated, covered, flat plate	30	water (and soil)	300	-9	-	10	4–8		Seasonal TES	[68]
Reuss et al., 2006 [104]	Attenkirchen, Germany 51°N	SH, HW	-	flat plate	764	water soil	500 6800 water equal	-	-	-	3.2–4.4		Seasonal TES	
Qi et al., 2008 [109]	Beijing, China 40 °N	SH	-	flat plate	30, 40, 50, 60	CaCl ₂	228, 456	-14.8	_	3.025	4.2		A serial/dual- source IX- SAASHP with seasonal latent TES	
Trinkl et al., 2009 [62]	Wuerzburg, Germany 50°N	HW, SH	-	covered, flat plate	30	water/ ice water	12.5 0.3–1	5	-	0.59 for SH and 0.23 for	-	4.6	-	
					34.38	water/ ice water	11 0.5			HW	-	4.7		
					24.83	water/ ice water	15 0.5				-	4.3		
Winteler et al.,	Wuerzburg,	HW, SH	_	bare	10	water/ice	10	_	_	1.09	_	4.25	_	
2014 [173]	Germany 50°N	-			13					1.74	_	4.47		
					20					2.26	_	4.12		
					30		20			3.59	_	3.73		
	Strasbourg,				10		10			0.6	_	3.73		
	France 48°N				10					1.11	_	4.23		
					20					2.31	_	4.02		
Cabonell et a. 2014 [90]	Strasbourg, France 48°N	SH, HW	-	bare and covered,	10–30	waste water water/ice	0.13 10–30	-	-	$0.005/\text{m}^2$	-	2–7	-	
				coated	20–40	waste water water/ice	0.13 20–50			$0.0114 / m^2$	-	2–4.5		
Carbonell et al.,	Strasbourg,	SH, HW	_	covered	15	ice	25	_	-	0.973	_	5.01	-	[98],[99,100]
2014 [82]	France 48°N			(including 5	20		20				-	5.53		
				m ² uncovered	30		20				-	5.90		
				collector)			40			1.147	-	4.78		
					45		30				-	5.1		
Li et al., 2014 [175]	Beijing, China 40 °N	SH, HW	_	flat plate	150	water	105	-6.5	-	_	6.2		Seasonal TES	
Qv et al, 2015 [95]	Shanghai, China 31.17°N	SC SH	R22	-	-	RT5HC	10.5 kg	30–43 –17	-	7.242 3.58	2.3–3 2.8	-	Using a novel triple-sleeve energy storage exchanger	[93,94,187]
Tamasauskas et al., 2015	Montreal, Canada 45°N	SC, SH, HW	R507a	covered, flat plate	11.9, 26.8	4% (by mass) propylene	5	_	-	0.935	-	2.53	_	[174]
[97]	Toronto, Canada 43.5°N					glycol/ water		-	-	0.863	-	2.55		
	Vancouver, Canada 49°N							-	-	0.767	_	2.43		

20

Table 5 (continued)

	Authors	Location	Function	Refrigerant	Solar collector		TES		T_a (°C)	$T_{\rm con}$	HC (kW)	COP	SPF	Comments	Related work
			of HP		type	area (m²)	type	volume (m³)		(°C)					
	Lerch et al., 2015 [46]	Graz, Austria 47°N	SH, HW	-	covered,	- 14	water water	0.3 1	-12	-	5.36	-	2.55 3.65	ASHP Hybrid SAASHP	[191]
					plate bare, coated	30	water	1				_	3.53	Serial IX-	
					bare, coated	30	water water/ice	1 0.6				-	3.56	SAASHP systems	
					covered, coated	14	water	1				-	3.68	A hybrid SAASHP using air preheated by solar as heat source	
					covered, coated	14	water	1				-	3.7	A dual-source IX-SAASHP	
3	Qu et al., 2015 [80]	Beijing, China 40°N	SH	-	vacuum tube	16.2	water Na ₂ SO ₄	0.85 0.8	-	-	-	10.03		-	
	Youssef et al., 2017 [81]	London, UK 51°N	HW	R134a	evacuated tube	3.021	water paraffin	0.3 30 kg	-	-	0.54–0.81	4.21–4.99		A serial/dual- source IX- SAASHP	
	Youssef et al., 2017 [244]	London, UK 51.5 °N	HW	-	evacuated tube	3.021	water	0.3	-	-	9.632	4.7			
	Han et al., 2018	-	SH, HW	-	evacuated tube	10	PCM PCM water	30 kg 510 kg 1	-23.4 - 20	-	0–45	0-8.3			
	Aktas et al., 2019 [223]	-	HW	R410A	double pass collector	-	paraffin RT42	-	-	60	-	3.3–3.8			
	Stritih et al., 2019, [225]	-	SH	R407C	evacuated tube	25	paraffin RT 31	-	-	-	-	4.3–5.7			
	Kutlu et al., 2020 [203]	-	HW	R134a	evacuated tube	4	water PCM	3 0.15	9–25	-	-	3.4–4.6			
	Lu et al., 2020 [249]	-	SH	_	-	40	water	40 2	-5-37	-	-	3.95 3.5	_	Seasonal TES Normal TES	

 Table 6

 Research on DX-SAASHP using flat plate collectors and water tank.

Authors	Location	Function of HP	Refrigerant	Solar collector	:	Volume of TES (m ³)	$T_{\rm a}$ (°C)	$T_{\rm con}$ (°C)	HC(kW)	COP	Related wor
		н		type	area (m²)	ies (m.)					
Chaturvedi and Shen, 1984 [33]	-	HW	R12	bare	3.39	-	-4-22	40–50	-	2–3	
Chaturvedi et al., 1998 [134]	Virginia, US 37.8°N	HW	R12	bare	3.48	-	10–27	40	1–1.5	2.5–4.0	[152,159]
Axaopoulos et al., 1998 [140]	Athens, Greece 38°N	HW	R12	bare	2	0.158	5–40	-	$0.14/m^{2}$	3.42	
Ito et al., 1999 [76]	Kanagawa, Japan 36°N	HW	R12	bare	3.24	-	8	-	-	5.3	
Huang and Chyng, 1999 [148]	-	HW	R134a	bare	1.57	0.12	31.3	45.6	-	3.83	
Huang and Chyng, 2001 [137]	Taiwan, China 23°N	HW	R134a	bare	1.44	0.105	27–37	45–68	0.678-0.926	2.5–3.7	[141]
Hawlader et al., 2001 [192]	-	HW	R134a	bare	3	0.25	26–36	-	-	4–9	
Torres-Reyes and Cervantes, 2001 [162]	Mexico 23°N	SH	R22	-	4.5	-	20–32	-	2.8–5.37	2.56–3.46	[163,164]
Chyng et al., 2003 [65]	Taiwan, China 23°N	HW	R134a	bare, coated	1.86	0.105	-	-	-	1.7–2.5	
Kuang et al., 2003 [70]	Shanghai, China 31.17°N	HW	R22	bare	2	0.15	3–12	-	-	4–6	
Ito et al., 2005 [146]	_	_	R22	_	1.91	_	_	_	_	4.5-6.5	
Chata et al., 2005 [151]	-	-	R12, R22, R134a, R404A, R407C, R410A	bare covered	15.6 17.2	-	5	60	7	3.8	
Kuang and Wang, 2006 [37]	Shanghai, China 31.17°N	SC, SH, HW	R22	bare	10.5	0.2, 1	7.9–12.1	-	5.8–7.6	2.1-2.7 (SH)	
Xu et al., 2006 [71]	Nanjing, China 32°N	HW	R22	bare	2.2	0.15	5	-	-	2.51–4.69	
Anderson and Morrison, 2007 [138]	Sydney, Australia 34°S	HW	R22	bare	4	0.27	25 20	-	-	5–7 3–5	
Huang and Lee, 2007 [142]	-	HW	R134a	coated	-	0.115 0.24 0.13	-	-	-	2.12–2.72 2.24–3.57 1.85–2.53	
Kara et al., 2008 [5]	Izmir, Turkey 38°N	SH	R22	none bare	4	0.2 -	2	55	1.75	2.48–2.78 –	
Mohanraj et al., 2008 [139]	Calicut, India 11°N	SH	R22	covered, coated	2	-	29–33.3	60	-	1.98–2.57	[145,147]
Chow et al. 2010 [32]	Hong Kong, China 22°N	HW	R134a	bare	12	2.5	30–32.8 13–15.8	58.1–63.5 51.65–55.85	4.82–6.3 3.52–5.33	6.57–10.7 4.31–9.14	
Kong et al. 2011 [73]	Shanghai, China 31.17°N	HW or SH	R22	bare	4.2	0.15	20.6–28.9	-	0.208-0.27	5.21–6.61	[72,74,87]
Fernández-Seara et al., 2012 [150]	-	HW	R134a	bare	-	0.3	7–22	21.2–57.9	-	3.23	
Moreno-Rodríguez et al., 2012 [143]	Madrid, Spain 40°N	HW	R134a	-	5.6	0.3	11–19	57	0.275-0.3125	1.7–2.9	
Moreno-Rodríguez et al., 2013 [144]	Madrid, Spain 40°N	SH	R134a	-	5.6	-	0–20	32–40	2.375–2.917	1.9–2.7	
Molinaroli et al., 2014 [136]	-	SH	R407C	bare	40.32 29.12 22.40	-	-5, 0, 5, 10, 15	50	7.5	2.2–4.3	

Energy Conversion and Management 247 (2021) 114710

Table 6 (continued)

Authors	Location	Function of	Refrigerant	Solar collector	r	Volume of	T_a (°C)	$T_{\rm con}$ (°C)	HC(kW)	COP	Related work
		HP		type	area (m²)	TES (m ³)					
					16.80						
Sun et al. 2014 [149]	Shanghai, China 31.17°N	HW	R134a	coated	1.92	0.15	26	-	-	4.5–8.5	[60]
Scarpa and Tagliafico, 2016 [61]	-	HW	R134a, R600a	bare	1	0.025	5.3, 16.5, 33.2	45	0.216, 0.295, 0.392	5.8	[155,156,158]
Deng and Yu, 2016, [34]	-	HW	R134a	-	2	0.15	-	55.1–57.6	_	4.46–4.74	
Paradeshi et al., 2016 [135]	Calicut, India 11.15°N	SH	R22	-	2	-	-	-	2.0–3.6	1.8–2.8	
Kong et al., 2017 [157]	_	HW	R410A	bare	4.2	0.15	25.7	_	3.14-4.27	3.62-8.6	[154]
Mohamed et al., 2017	-	SH, HW	R407C	bare	4.22	0.2	6.5–8.5	86	3.3–4.2	2.7–3.9	
Paradeshi et al., 2018 [234]	Calicut, India 11.15 °N	SH	R22, R433A	covered	2	-	-	-	1.9–3.5	-	
Cai et al., 2019 [29]	_	HW	_	bare	4.2	0.15	5–15	31-50	1.5-2.5	2.5-3.5	
Huang et al., 2019 [213]	-	SH	_	bare, coated	4	-	-5-5	-	0.75–1.1	1.5–2	
Duarte et al., 2019 [230]	Pampulha, Brazil	HW	R134a, R290, R600a, R744, R1234yf	coated	1.65	0.2	25–33	-	-	2.25–2.91	
Rabelo et al., 2019 [242]	-	HW	R134a, R290	uncovered	1.65	0.2	25	60, 65, 70	1.37	2.5	
Cao et al., 2020 [237]	_	HW	R134a	covered	4.2	0.15	25.7	_	_	4–6	
Cai et al., 2020 [215]	-	SH	_	bare, coated	4	-	2–15	-	2.4–2.7 parallel; 2.35–2.6 serial	4.5–4.58 parallel;4.33–4.5 serial	
Liu et al., 2020 [243]	Qinghai, China 36 °N	SH	R22	-	6	1.8	-3.1	45	_	2–4	
Zhang et al., 2020 [216]	Hefei, China 32 °N	SH, SC	_	bare, coated	-	0.3	5.9–14	-	_	2.87–3.8	

Table 7
Research on IX-SAASHP and hybrid SAASHP using flat plate collector and water tank.

Authors	Location	Function	Refrigerant	Solar colle	ector	Volume of	T_a (°C)	HC (kW)	COP	SPF	Relate
		of HP		type	area (m²)	TES (m ³)					work
Freeman et al., 1979 [63]	Madison, US 43°N Albuquerque, US 35°N Charleston, US 38°N	SH, HW	-	-	10, 20, 30, 40, 50, 60	0.075 per m² solar collector	-	1.95 (SH), 0.68 (HW) 0.94 (SH), 0.68 (HW) 0.485 (SH), 0.68 (HW)	2 (hybrid) 2.5 (dual-source) 2.8 (serial)	-	
umrutas and Kaska, 2004 [42]	Gaziantep, Turkey 37.18°N	SH	R22	covered	7.4	0.65	7.8–16.1	-	2.5–3.5	-	
Dikici and Akbulut, 2008 [75]	Elazig, Turkey 38.41°N	SH	R22	-	11.1	0.18	3.9	3.844	3.08	-	[49]
i and Yang, 2009 [161]	-	HW	R22	-	6	0.4	15–30	11	4 (DX- SAASHP), 4 (serial),3 (hybrid)	-	
Chaichana et al., 2010 [166]	Chiang Mai, Thailand 18.8°N	HW	R22:R124: R152a (20%: 57%: 23%)	bare	4, 8, 12, 16, 20	0.3, 0.6, 0.9, 1.2	13.7–36.2	-	4.1–4.6	-	[168]
i and Yang, 2010 [43]	Hong Kong, China 22°N	HW	R22	covered	390	32	15 25	-	3.5 3.86	-	
Sakirci and Yuksel, 2011 [41]	Erzurum, Turkey 41°N	SH	R134a	coated, covered	1.64	2	-10.86	3.801	2.86	-	
terling and Collins,	Ottawa, Canada 45°N	HW	-	-	4	0.5	-	0.634	2.5–5	-	[53]
2012 [54] agliafico et al., 2012 [178]	-	HW	-	bare	1.78	-	0–15	150	-	-	
Thow et al., 2012 [165]	Hong Kong, China 22°N	SH, HW	R22	-	1400	-	10–23	-	4.48–4.56	-	
anaras et al., 2014 [183]	Athens, Greece 23.5°N	HW	-	coated	2.58	0.28	18.5	0.643	2.12	-	[180]
anister and Collins, 2015 [169]	-	HW	-	_	2.5, 5, 7.5, 10	0.3, 0.45	_	-	2.3–6.3	-	
Fraga et al., 2015 [167]	Geneva, Switzerland 46°N	SH, HW	-	bare	116	6 + 0.3*8	-2.4-20.5	2.13 (SH), 5.28 (HW)	-	2.9	[229]
i et al., 2015 [186]	Lab based	HW, SH, SC	-	-	3.2	0.2	7	1.2–2.4 (HW) 1.4–2.2 (SH)	1.75–3 (HW) 2.35–2.75 (SH)	-	
Cai et al., 2016 [44]	Lab based	SH, SC, HW	-	-	3.2	0.3	7	1.9–2.4 (HW) 1.3–1.5	2–3.25 (HW) 2.25–2.5 (SH)	-	[214]
oppi et al., 2016 [185]	Zurich, Switzerland, 47°N	SH, HW	R410A	-	9.28	0.763	-10	(SH) 0.347 (HW), 0.944 (SH)	-	3.16	[184]
								0.347 (HW), 1.966 (SH)	-	2.43	
	Carcassonne, France 43°N						-5	0.307 (HW), 0.419 (SH)	-	3.85	
								0.307 (HW), 1.047 (SH)	-	2.93	
iu et al., 2016 [50]	Zhengzhou, China 34°N	HW, SH	-	-	-	-	-15, -10, $-7, -5, 2, 7$	1.2–2.9	2–3.1	-	
i and Kao, 2017 [182]	Taipei, China 25°N Kaohsiung,	HW	R410A	-	3.84	0.46 0.92 0.46	-	-	- - -	3.92 4.36 4.31	
Bellos and Tzivanidis, 2017 [176]	China 22.5°N –	SH	-	-	5–80	0.92 1	-1.4-14	5–15	4	4.83 -	
2017 [176] Li and Kao, 2018 [240]	-	HW	_	-	5		4–30	-	-	-	

(continued on next page)

Table 7 (continued)

Authors	Location	Function	Refrigerant	Solar colle	ector	Volume of	T_a (°C)	HC (kW)	COP	SPF	Relate
		of HP		type	area (m²)	TES (m ³)					work
						0.4 + 0.2, 0.5 + 0.25, 0.6 + 0.3					
Ran et al., 2020 [231]	Lhasa, China	SH, HW	-	-	300	10	-	120	-	6.92	
	Chengdu, China							90	_	3.61	
	Beijing, China							180	_	3.27	
	Shenyang China							270	-	2.45	
Liu et al., 2020 [238]	Chongqing, China 29 °N	HW	R410a	-	5.5	0.25	5–40	-	2–5.2	-	
Wang et al., 2020 [233]	Changsha, China 28.5 °N	HW	R134a	covered	150	10	20–30	-	1.5–3.5	-	
Long et al., 2021 [211]	-	HW	_	-	12	0.3	26–32	3–11	1.5–5.5	-	

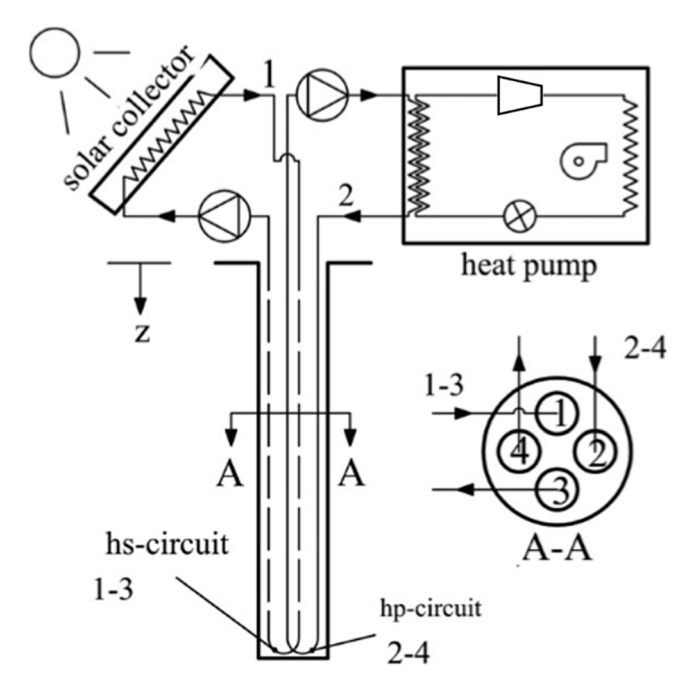


Fig. 22. Solar-geothermal hybrid source HP (reproduced from [84]).

from air and thus increase efficiency.

The required output temperature has a negative linear influence on *COP*. As Fig. 30 shows, a study of a DX-SAASHP for HW concluded that the higher the output water temperature was, the lower system *COP* would be [35,65,70,137]. As the output water temperature increases from 25 °C to 60 °C, the *COP* drops from 3.7 to 2.7 linearly. An experiment of a DX-SAASHP for HW shows that, with a rise of temperature difference between output water and ambient environment from 5 °C to 40 °C, *COP* drops from 5 to 2 (see Fig. 31) [138]. This is, as output water temperature increases, compressor discharge pressure increases, and therefore energy consumption increases [44]. In turn, as inlet source temperature decreases, compressor suction pressure decreases. The increase in pressure ratio brings lower *COP*.

Fig. 32 summarises the effect of ambient temperature on *COP* of the SAASHPs for different end use in published papers. The advanced systems refer to the SAASHPs involving innovations in the aspects of solar collector, TES and system configuration. In this figure, the *COP* values are taken the average values and the ambient temperatures are taken the lowest values of the working conditions. The ambient temperature ranges from $-15~^{\circ}\text{C}$ to 30 $^{\circ}\text{C}$ and *COP* ranges from 2 to 8.5. Majority of the *COPs* obtained ranges from 2 to 6. Especially, an IX-SAASHP for SH using seasonal latent heat TES earned a *COP* of ca. 4.2 at $-15~^{\circ}\text{C}$ [109]. Similarly, another IX-SAASHP with seasonal TES for SH achieved higher *COP* of ca. 8.5 with a collector area of 40 m² and a storage volume of 1960 m³ [68]. Interestingly, the *COP* values of two DX-SAASHPs shown in [32] and [139] vary significantly. This concerns many reasons. The DX-SAASHP in [32] uses R134a as the working fluid and uses an

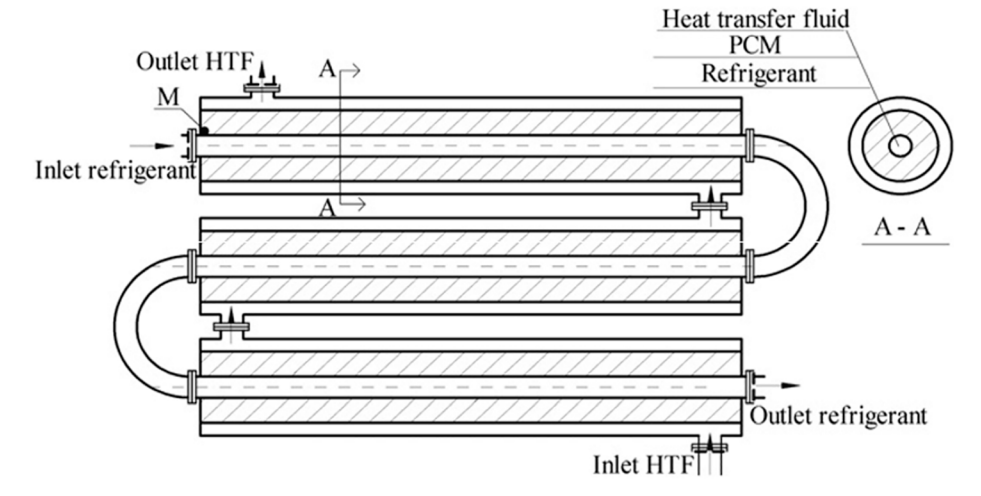


Fig. 23. Triple-sleeve heat exchanger [93].

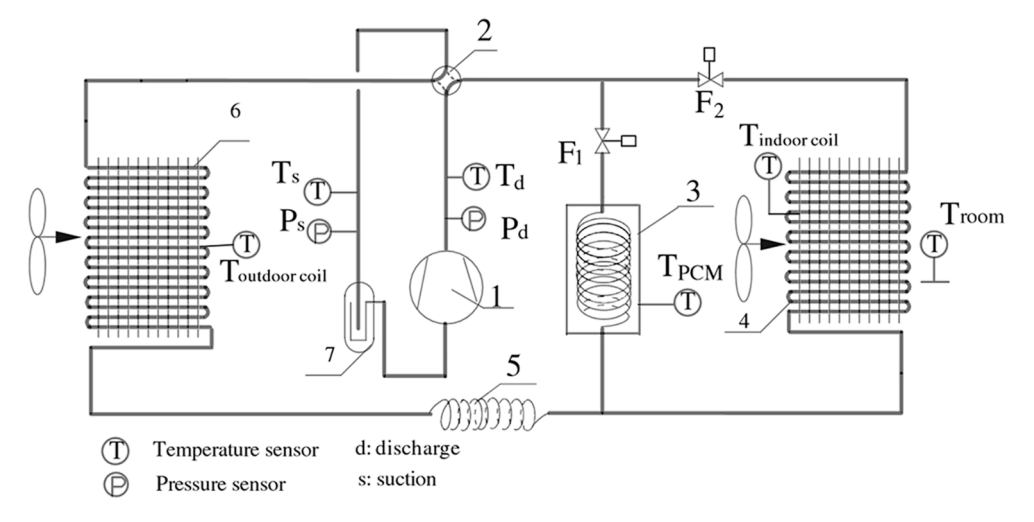


Fig. 24. Reverse-cycle defrosting ASHP system with energy storage [121,122].

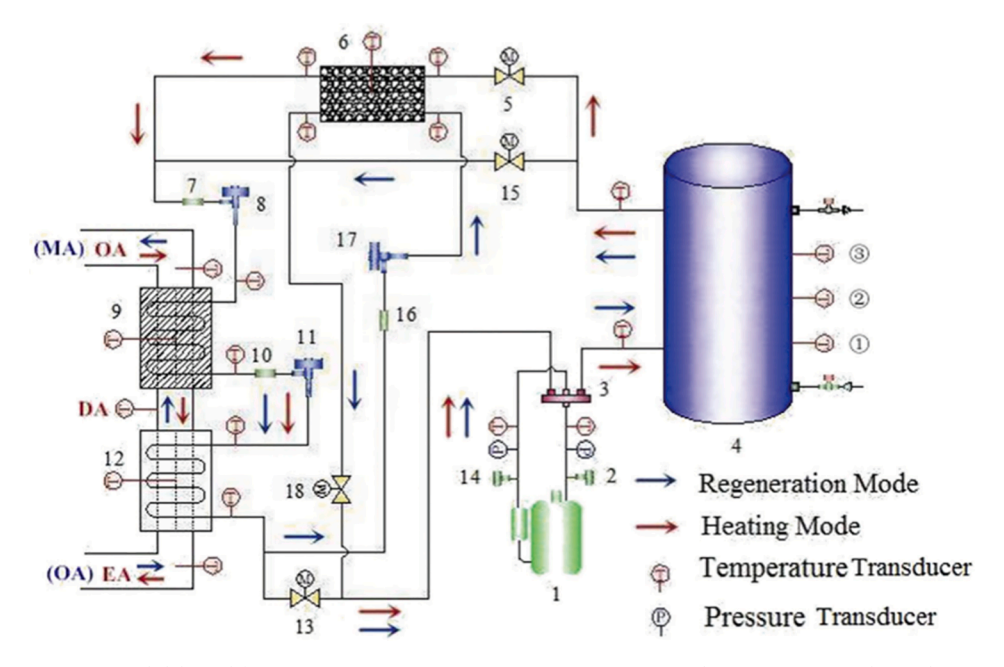


Fig. 25. ASHP with energy storage and dehumidification [124,125]. 1 - compressor, 4 - water TES tank, 6 - PCM TES tank, 9 - desiccant-coated evaporator, 12 - evaporator.

uncovered collector of 12 m^2 ; the DX-SAASHP in [139] uses R22 as the working fluid and uses a covered collector of 2 m^2 . Overall, advanced IX-SAASHP is ideal for SH as well as HW, and DX-SAASHP is more suitable to HW. For multi-functional SAASHP, advanced IX-SAASHP is the best choice.

Fig. 33 summarises the number of open literature having different *COP* where *COP* values take the average of values given in the studies. It can be observed that the *COP* values of most of these SAASHPs are located in the range from 2.0 to 6.0. The dual-source IX-SAASHP achieves *COP* lower than 3.5. The hybrid SAASHP, serial IX-SAASHP, advanced DX-SAASHP and dual-source DX-SAASHP can achieve *COP* less than 6. Both the DX-SAASHP and advanced IX-SAASHP can achieve *COP* higher than 6, promisingly up to 10.5. Considering economic aspect, DX-SAASHP and hybrid SAASHP shares similar payback period for around 4.5 years, while the payback period of serial IX-SAASHP is around 7 years [161].

It can be concluded from the above that solar collector and thermal energy storage have significant influence on the system performance. The influences are displayed in Fig. 34, where the solid line represents the SPF and the dashed line represents the yearly electricity consumption, that larger collector area and storage volume lead to a higher SPF and lower electricity consumption [76,96,135,192]. According to Ito et al.'s [76] and Carbonell et al.'s [90] simulations, uncovered collectors are superior to covered collectors with a collector area lower than 15 m². For larger collector area, covered collector with proper storage volume can help to achieve an SPF over 6. Small-scale SAASHPs for the domestic sector require high-efficient solar collectors to reduce collector area at the same SF and working conditions. This may be achieved by auxiliary components, such as compound parabolic concentrator [55,57,58,108]. Xu et al.'s [108] simulation revealed that a collector using compound parabolic concentrator and capillary tube absorber can achieve higher collecting temperature and higher collector efficiency than that of a flat plate collector at the same size. According to Ito et al. [76], collector plate thickness and tube pitch can affect system SPF according to plate material and ambient temperature. Larger plate thickness and lower tube pitch result in higher SPF. Simulation of an uncovered collector

Energy Conversion and Management 247 (2021) 114710

Table 8
Advanced SAASHP systems.

Authors	Function of HP	Refrigerant	Solar collector		Volume of	T_a (°C)	$T_{\rm con}$	HC	COP	Comments
			type	area (m²)	TES (m ³)		(°C)	(kW)		
Chaturvedi et al., 2009 [36]	-	R134a	covered	10.58 8.77	-	5	60 90	-	-	A two-stage DX-SAASHP for high temperature applications
Li et al., 2013 [179]	HW SH SC	-	-	11.4	3	-10-34 -10-18 26-34	-	-	1.4–4.4 3.6–6.7 1.2–23	A wind-powered hybrid SAASHP A wind-powered serial IX-SAASHP
Lv et al., 2015 [52]	HW	R32/R290 (20%/80% by mass)	_	_	_	_	55	_	3.84	A solar assisted auto-cascade HP
Faria et al., 2016 [56]	HW	CO ₂	-	1.57	_	30	-	-	_	A trans-critical DX-SAASHP
Yan et al., 2016 [39]	HW	R134a, R1234yf	-	2	-	25	55	2.43	4.07	A vapour ejector enhanced DX- SAASHP
Chen and Yu, 2017 [40]	HW	R134a	-	5	-	-	40–75	-	4.61–5.61	A vapour ejector enhanced DX- SAASHP
Chargui and Awani, 2017 [212]	SH	CO_2	bare	8	2	10-20	-	2.5-6	3.4-5.5	
Chen and Yu, 2018 [227]	HW	-	_	5	_	_	40-70	6-6.5	3.5-6.5	An ejector enhanced DX-SAHP
Qiu et al., 2018 [210]	HW	-	-	20	-	-25-10	50	10–14	2–2.9	A cascade serial IX-SAASHP and two two-stage dual-source DX- SAASHP
Rabelo et al., 2018 [218,232,246]	HW	CO ₂	bare, coated	1.57	0.2	25	-	1.4–1.9	3–5.5	A trans-critical DX-SAASHP
Chen et al., 2019 [228]	HW	R134a	-	-	0.1	-	-	1.9–2.7	2.3–5.8	An ejector enhanced DX-SAASHP using micro-channel condenser
Fan et al., 2019 [226]	HW	R290/R600a	_	_	_	-20-20	_	_	2.5-7.5	An ejector enhanced DX-SAHP
Yerdash et al., 2020 [51]	HW, SH	R134a/R410a, R32/R290, R32/R1234yf, R32/R134a, R410A/R290, R410/R1234yf, R744/R290, R744/ R1234yf, R744/R134a	-	6	0.3	-30-10	40–60	-	1.8–3	A solar assisted cascade HP
Kong et al., 2020 [127,193,194,196,198,199]	HW	R134a	bare	2.1	0.2	-3-7	20–45	-	2.72-4.16	Using micro-channel condenser
Ma et al., 2020 [245]	SH	CO ₂ , R410a	-	70	3	-6.6 - 12.7	35	-	_	A two-stage serial IX-SAASHP

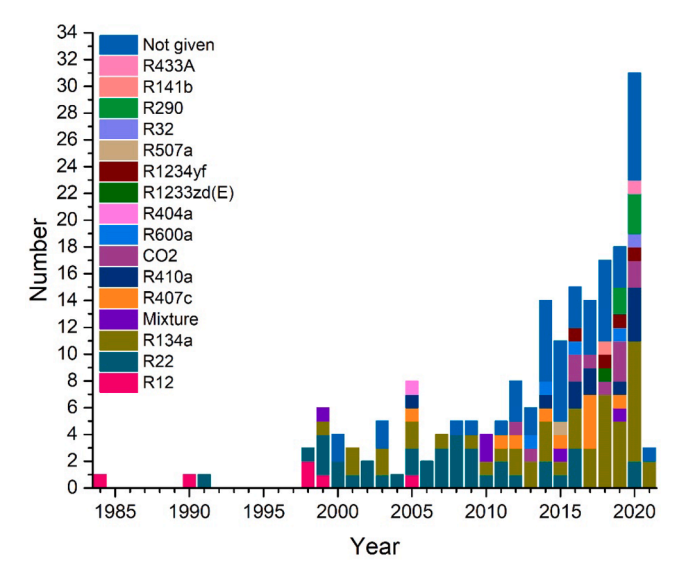


Fig. 26. Number of papers published in journals per year for SAASHPs using different refrigerants.

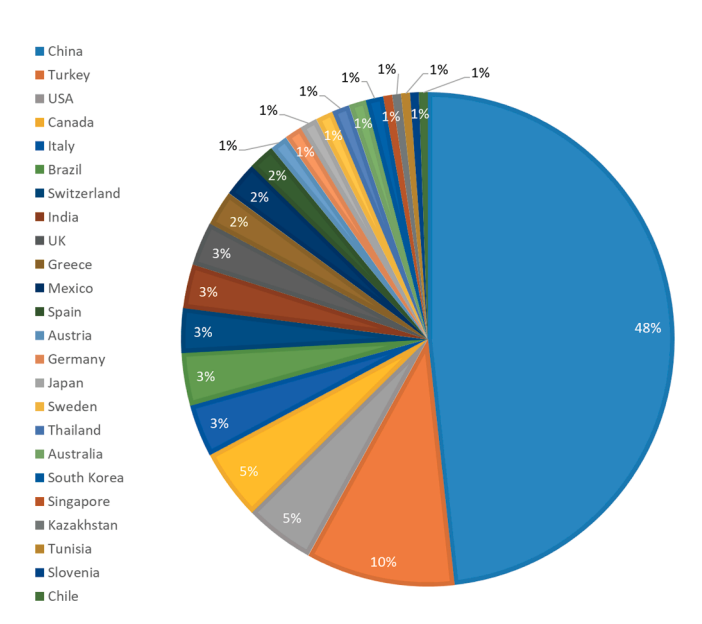


Fig. 27. Distribution of investigations in countries.

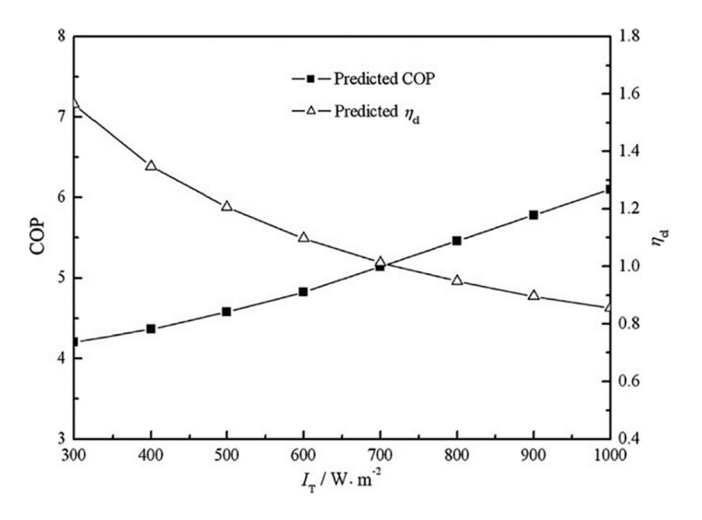


Fig. 28. Effects of solar irradiance $I_{\rm T}$ on *COP* of the SAASHP and the collector efficiency $\eta_{\rm cl}$ [73].

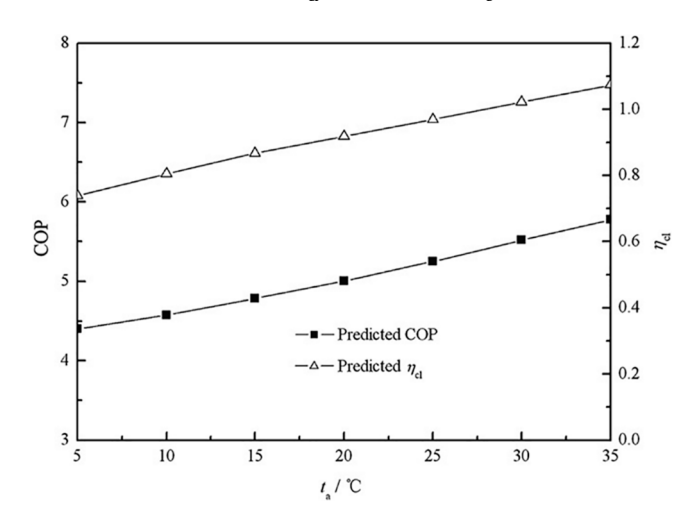


Fig. 29. Effects of ambient temperature $t_{\rm a}$ on COP and collector efficiency $\eta_{\rm cl}$ [73].

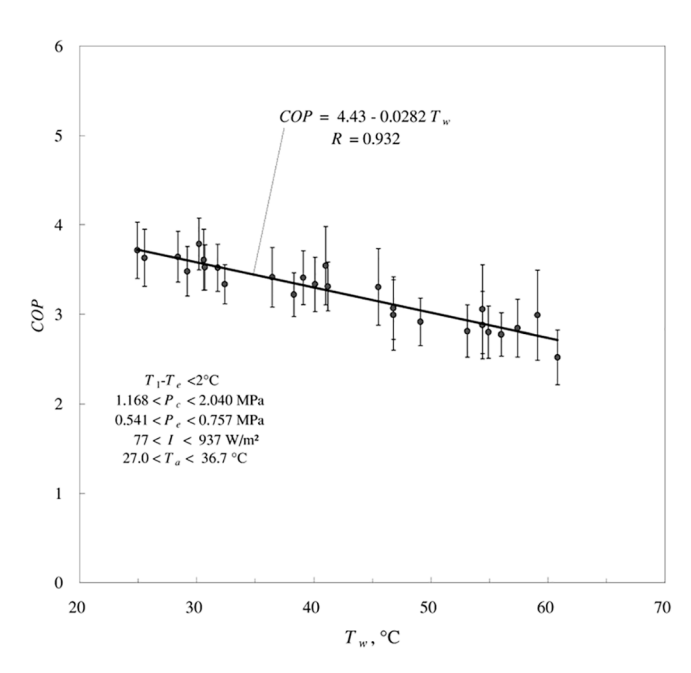


Fig. 30. Effect of output water temperature $T_{\rm w}$ on *COP* [137].

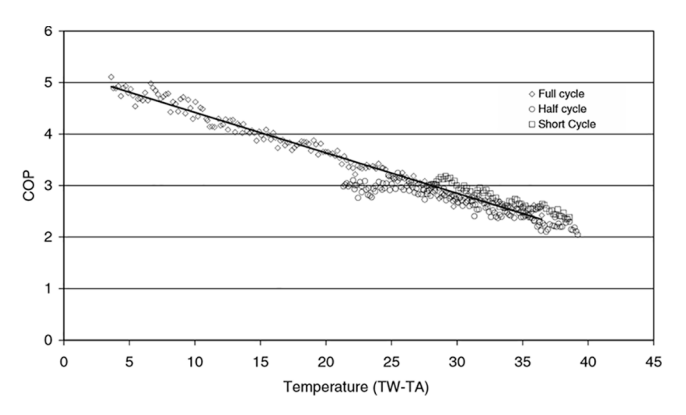


Fig. 31. COP as a function of the temperature difference between average water temperature in water tank to ambient air, T_{w} - T_{a} [138].

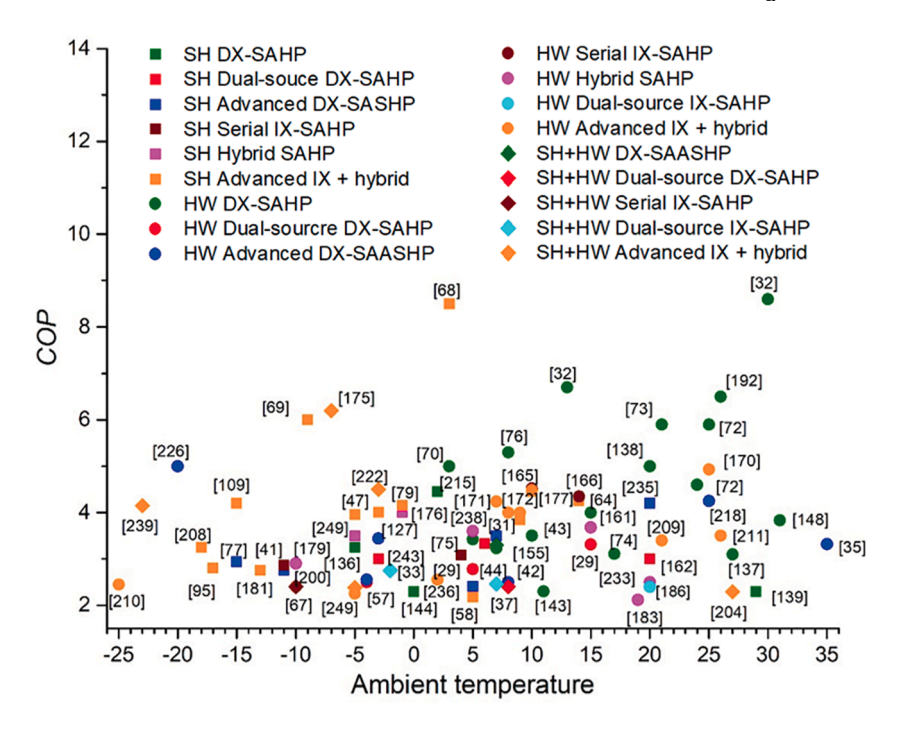


Fig. 32. COP vs ambient temperature of the SAASHPs for SH and HW.

suggested that the influence of plate thickness is apparent at smaller thickness and tends to be less at larger thickness. Other parameters such as inclination angle of solar collectors hardly affect *SPF* and collector efficiency [41,108].

Current studies on solar collectors mainly adopt the collectors designed for solar domestic HW. The specific collectors for SAASHP are needed to be developed, which should match the development of TES methods and the requirements of the SAASHP. Currently, for most systems using sensible heat TES, solar collector is expected to achieve higher outlet temperature to store more thermal energy in the same storage volume. In the future, as PCM is adopted to improve TES efficiency and combined with defrosting for the smooth operation of systems with evaporator, e.g., hybrid SAASHP, the required collector outlet temperature can be lower, just above the phase change temperature. A novel control strategy proposed by Xu et al. can be used to control the fluid flow rate and outlet temperature of solar collectors based on

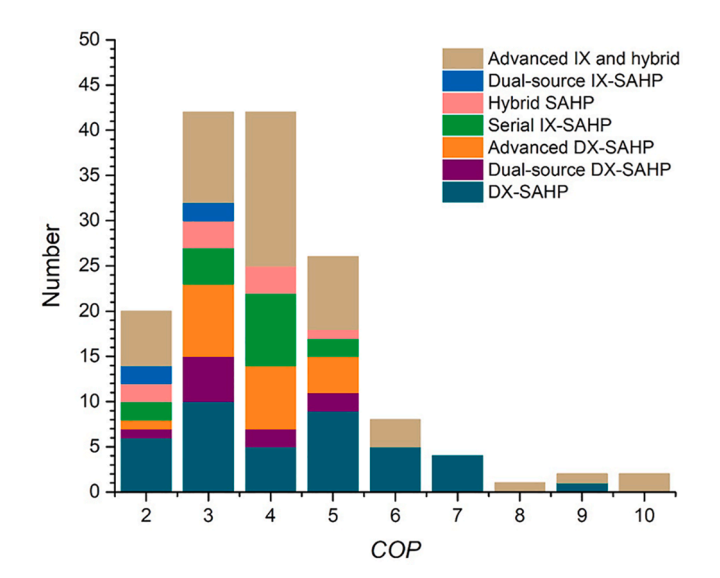


Fig. 33. Number of journal papers vs COP.

working conditions, enabling optimization of SAASHPs [188].

Increasing investigations of SAASHPs are seen in the most recent years. Great efforts have been put to develop high efficient and compact components to match the working conditions of SAASHPs and hence to improve the system performance. Particularly, eco-friendly refrigerants such as R1234yf, R1233zd(E), R433A, R32 and R290 are used to deal with the global warming.

7. Potential and barriers

The world is actively decarbonizing the energy sector through the development, first, of the renewable electricity and the abandonment of hydrocarbon combustion based systems. HPs are of the greatest interest. Combining and hybridizing solar thermal collectors with HPs can significantly increase the performance of the system. The COP of HPs has increased substantially over the past years due to technical improvements. The integration of solar thermal energy will boost the COP even higher. According to IEA recent report on Solar Heating and Cooling Programme, in 2019 solar thermal systems provided 479 GW thermal energy. This is equivalent to save 43 million tons of oil and to avoid 138 million tons of CO_2 emissions [189].

In Europe and the UK are trying to standardize and commercialize SAHPs. For example, companies, such as Solamics Bunsen Air, mainly focused on DX-SAHP water heaters. As an evaporator in such DX-SAHP, so-called thermodynamic panel or roll-bond evaporator is used. This is simply an unglazed absorber plate of solar thermal collectors, which is shown in Fig. 20 as a collector/evaporator. The main shortcoming of such evaporators is a huge heat loss due to non-glazing and isolation, but this is also an advantage, since in the absence of solar radiation, natural convective heat exchange with ambient air allows the evaporation process. With a high solar radiation intensity in the collector/evaporator, the refrigerant turns into a gaseous phase with large volumetric and superheating conditions, which may cause overheating of compressors with further mechanical failure. Therefore, finding efficient DX dual-source [38] configurations with forced convection type fan-coil evaporator assistance is of interest for further research. At the same time, there is a need for adaptation to specific climate conditions, taking into account the meteorological and consumer demand boundary conditions. This, in turn, leads to an optimal selection of other components,

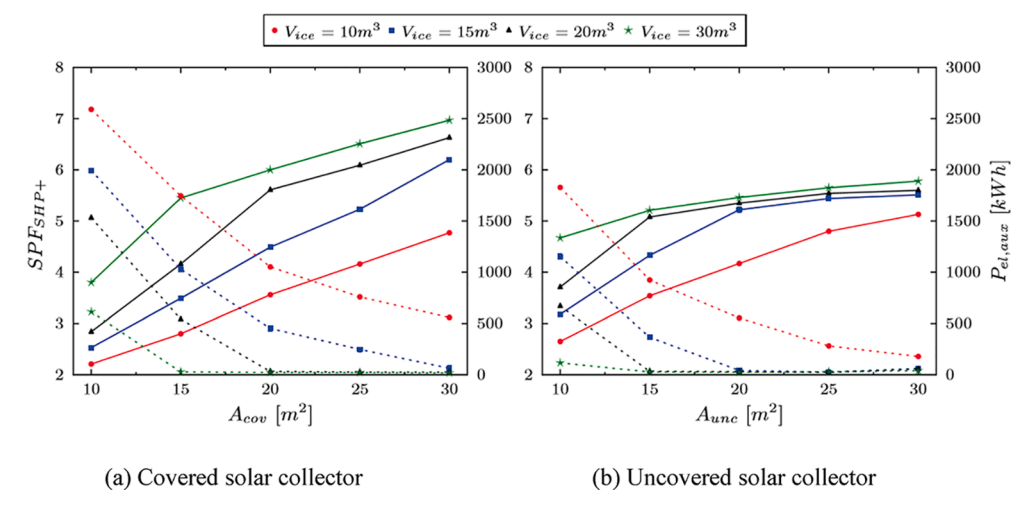


Fig. 34. SPF and yearly auxiliary energy as function of ice storage volume and solar collector area for building SFH 45 [90].

such as a compressor, expansion valve and condenser.

In IX systems comprehensively discussed in section 2.2 solar thermal collectors are connected with vapor compression heat pump cycle through the water storage tank or intermediate heat exchanger. In this case, a heat pump of the "Water-Water" type is used, the evaporator and condenser of which is a brazed plate heat exchanger. In this case, the heat transfer fluid flows in solar collectors without phase changing. In this configuration, the processes in solar thermal part are more controllable and predictable. The use of solar collectors and air source evaporators in the SAASHP system can be dual-source IX-SAASHP or hybrid SAASHP. In the configurations presented in section 2.2 and 2.3, the fan-coil evaporator is mainly used in the refrigerant circuit. Few studies are presented for an air source evaporator in a hydraulic circuit, where heat exchange occurs without phase changing. The search for the most optimal configuration for IX-SAASHP taking into account automated components and bringing it to the level of commercialization is the interest of the authors of the present review, in particular for UK case.

Automation implies the use of electronic components instead of mechanical ones with an appropriate control algorithm and the use of sensors. An intelligent control algorithm for an automated system will allow systems to work with the highest efficiency, of course, after determining the efficient configuration of the DX-SAASHP and IX-SAASHP based on thermodynamic calculations and experiments. In this regard, varible frequency drive (VFD) compressors and electronic expansion valves are of interest, which separate the high and lowpressure sides of the vapor compression cycle. In heating, ventilation and air-conditioning systems, the VFD can be used in fans, pumps and compressors with variable loads. VFD compressors are of particular interest for DX types of the vapor compression cycle both solar and ambient air since intermittent nature of solar irradiation and variability of ambient air temperature. Due to the variability of the weather boundary conditions, the volumetric flow rate of the vaporous refrigerant through the DX evaporator will be different and, accordingly, the VFD will control the volumetric efficiency of the compressor. By adjusting the frequency of the electrical power supplied to the compressor motor, the VFD controls the rotational speed of the alternating current motor. The energy savings for compressors up to 35% in heating, ventilation and air-conditioning systems [190]. In low solar irradiation or ambient air temperature, which affects evaporation temperature the heating capacity of a heat pump decreases. Similarly, heat pumps with VFD compressors allows adjusting the heating capacity in the different ranges with appropriate frequency. Obviously, the highest COP will be obtained for the lowest frequency. The COP value decreased proportionally to the increase in condensing temperature.

The issues of finding the optimal configuration and studying the optimal operation of DX-SAASHP and IX-SAASHP, taking into account the use of high-tech components such as VFD compressors/pumps/fans, electronic expansion valve, compact brazed heat exchangers are still open for specific climate conditions. At the same time, for significantly low outside temperatures, research is also needed on the application and optimal use of the auxiliary heater. This will entail research in the field of control and monitoring, the development of an optimal algorithm and system controller. There is a lot of research potential in this regard, but there are some barriers associated with mass commercialization.

Insufficient recognition of the benefits and high investment costs are the main barriers to widespread use of HPs. Also, in some countries with comparatively low energy prices (natural gas, electricity, etc.), in particular, resource-rich countries, HP operating costs are also inferior to conventional heat supply. In these countries, it is necessary to revise the tariff policy taking into account international environmental protection standards. Defining international standards for HP efficiency, optimization of system and components performance, local production and assembling of the entire system and individual details may be of interest to many representatives of small and medium-size enterprises, start-ups, service engineers, manufacturers and suppliers of heating, ventilation and air conditioning equipment. There is a much progress in conventional ASHPs and GSHPs, meanwhile for SAHP systems, including DX-SAASHP and IX-SAASHP, these actions are at the initial

In terms of environmental protection, in regions with a predominant demand for heat supply, during the heating season in large cities and towns there is a poor air quality due to emissions from energy facilities. This leads to a sharp increase in respiratory and allergic diseases. The transition to clean heat provision technologies is the policy of the administration of many cities and towns. In this regard, the technology of heat provision of residential and commercial buildings, individual households using solar thermal energy and ASHP may be of interest to eco researchers, local executive bodies, cities administration, energy policy and decision makers, environmental activists and communities. Therefore, energy policy and decision makers should propose incentive mechanisms in the form of subsidies, grants, etc. to accelerate the transition to clean heat supply technologies like the SAASHP.

New constructions of the building sector are responsible for the most of HP purchases. In the US, for example, the share of HP sales for new buildings is about 50% for new multi-family buildings and is higher than 40% for single-family dwellings [1]. The European Union, Japan and China markets are expanding quickly. The HP market size is huge even for new buildings. However, to boost adoption in existing buildings across the globe, it is necessary to work to remove the abovementioned

technological and economic barriers. In summary, SAASHP has demonstrated advantages and perspective for domestic space heating and hot water. To increase the uptake of SAASHPs, innovative design and optimization of components and system are needed to improve the performance of the system, to reduce the costs and to ensure its robustness of operation.

8. Conclusions

The integration of solar thermal energy and an ASHP based on vapour compression cycle is the subject of study by many researchers and a review of the recent research and developments has been presented in this article. Five typical and five advanced type solar SAASHPs have been analyzed. Three solar thermal collector types and three thermal energy storage methods have been discussed. Ten defrosting methods have been briefly discussed.

The investigations so far have demonstrated that the SAASHP is a promising technology for HW and SH in the domestic sector. SAASHPs in the domestic sector are mainly investigated by researchers from midlatitude (20°-50°) countries where SH is required in winter and HW throughout the year under the medium solar irradiance and temperate climate conditions (-15 °C - 30 °C). In the future, multi-functional SAASHPs as well as SAASHPs for high-latitude areas need to be further investigated by developing advanced IX-SAASHP with enhanced solar collector and TES method.

The *COP* values of most SAASHPs are ranging from 2 to 6. The dual-source IX-SAASHP achieves *COP* lower than 3.5. The hybrid SAASHP, serial IX-SAASHP, advanced DX-SAASHP and dual-source DX-SAASHP can achieve *COP* up to 6. Both the DX-SAASHP and advanced IX-SAASHP demonstrate their promising potential, enabling *COP* higher than 6 and up to 10. Advanced IX-SAASHP is ideal for SH and HW, and DX-SAASHP is better suitable to HW. Current studies on SAASHP focus on the matching and optimisation of system configuration. However, the optimisation of each component and its matching application in SAASHP should be further considered.

Current studies on solar collectors mainly adopt the collector designed for solar domestic HW. For flat plate collector, the uncovered solar collectors are superior to covered solar collectors at the collector area less than 15 m^2 . Small-scale SAASHPs for the domestic sector require high-efficient solar collectors, which may be achieved by auxiliary components such as concentrator.

The development of specific collectors for SAASHP should match the development of TES methods. The latent heat TES brings better storage and system performance over sensible heat TES, although latent heat TES is not economical yet. Basically, solar collector is expected to collect more solar energy to improve SAASHP's COP and SPF. Currently, for common SAASHPs using sensible heat TES, solar collector is expected to achieve higher outlet temperature to store more thermal energy at the same storage volume. Seasonal storage of surplus solar thermal energy is most suitable for a GSHP with underground storage in the form of a borehole TES, aquifer TES or a buried water tank in the ground (PCM). For SAASHP, short-term thermal energy storage in an HW storage tank for daily use is suitable, in particular, enhanced by PCM. In the future, as PCM is developed to improve the efficiency of TES and combined with the defrosting method for the smooth operation of systems with evaporator i.e. hybrid SAASHP, the collector outlet temperature should be above the phase change temperature.

Further studies are needed to improve the defrosting process. In component level, the material or the structure of the air source evaporator can be optimised to prevent or reduce the freezing process. In system level, optimisation on system configuration is also a potential approach for dual-source IX-SAASHP and hybrid SAASHP.

Currently, refrigerants (e.g. R22, R134a, R410A and R407C) are widely used in HP systems due to their good thermodynamic and thermophysical properties. R32 is a more environmentally friendly alternative refrigerant for R410A in ASHP. However, it is classified as a

flammable refrigerant A2L and therefore some countries are researching other retrofits, such as R454B. Therefore, future studies should concentrate more on the applications of environmentally friendly refrigerants in SAASHPs responding to global restrictions.

The outcome of this review is expected highly beneficial and valuable to the academia and engineers working with SAASHP systems, the HP/solar collector manufacturers and suppliers, installers and service workers, policy makers and energy experts.

Declaration of Competing Interest

The authors declare that they have no known competing financial interests or personal relationships that could have appeared to influence the work reported in this paper.

Acknowledgements

Funding: This work was supported by the Engineering and Physical Sciences Research Council (EPSRC) of the UK [EP/N020472/1]; the Royal Society of IEC\NSFC\170543-International Exchanges 2017 Cost Share (China); the Joint PhD Studentship of China Scholarship Council (CSC) and Queen Mary University of London; the National Natural Science Foundation (NSFC) of China [51506004]; the Project APP-SSG-17/0280F jointly funded by Science Committee of Kazakhstan Education and Science Ministry and World Bank.

References

- International Energy Agency. https://www.iea.org/reports/heat-pumps. [accessed 10 September 2020].
- [2] Department of Energy and Climate Change Statistics. Special feature estimates of heat use in the UK. 2014. https://assets.publishing.service.gov.uk/government/uploads/system/uploads/attachment_data/file/386858/Estimates_of_heat_use. pdf. [accesses 11 September 2020].
- [3] Department for Business, Energy & Industrial Strategy. 2050 Pathways Analysis. 2010. https://assets.publishing.service.gov.uk/government/uploads/system/uploads/attachment_data/file/68816/216-2050-pathways-analysis-report.pdf. [accessed 11 September 2020].
- [4] Demir H, Mobedi M, Ülkü S. A review on adsorption heat pump: problems and solutions. Renew Sustain Energy Rev 2008;12:2381–403.
- [5] Kara O, Ulgen K, Hepbasli A. Exergetic assessment of direct-expansion solarassisted heat pump systems: review and modeling. Renew Sustain Energy Rev 2008;12:1383–401.
- [6] Omojaro P, Breitkopf C. Direct expansion solar assisted heat pumps: a review of applications and recent research. Renew Sustain Energy Rev 2013;22:33–45.
- [7] Amin ZM, Hawlader MNA. A review on solar assisted heat pump systems in Singapore. Renew Sustain Energy Rev. 2013;26:286–93.
- [8] Facao J, Carvalho MJ. New test methodologies to analyse direct expansion solar assisted heat pumps for domestic hot water. Sol Energy 2014;100:66-75.
- [9] Shi GH, Aye L, Li D, Du XJ. Recent advances in direct expansion solar assisted heat pump systems: a review. Renew Sustain Energy Rev 2019;109:349–66.
- [10] Ruschenburg J, Herkel S. A review of market-available solar thermal heat pump systems: a technical report of subtask A'. 2013. http://task44.iea-shc.org/data/sit es/1/publications/T44A38-SubA-Report1-1305031.pdf. [accessed 11 September 2020].
- [11] Ruschenburg J, Herkel S, Henning HM. A statistical analysis on market-available solar thermal heat pump systems. Sol Energy 2013:95:79–89.
- [12] Frank E, Haller M, Herkel S, Ruschenburg J. System classification of combined solar thermal and heat pump systems. Proceedings of the EuroSun 2010 Conf. Graz, Austria.
- [13] Ozgener O, Hepbasli A. A review on the energy and exergy analysis of solar assisted heat pump systems. Renew Sustain Energy Rev 2007;11:482–96.
- [14] Haller MY, Bertram E, Dott R, Afjei T, Ochs F, Hadorn JC. Review of component models for the simulation of combined solar and heat pump heating systems. Energy Procedia 2012:30:611–22.
- [15] Chu J, Cruickshank CA. Solar-assisted heat pump systems: a review of existing studies and their applicability to the Canadian residential sector. In: Proceedings of the 7th Int Conf on Energy Sustainability Collocated with the ASME 2013 Heat Transfer Summer Conf and the ASME 2013 11th Int Conf on Fuel Cell Sci, Engineering and Technology. Minneapolis, Minnesota, USA. 2013.
- [16] Kamel RS, Fung AS, Dash PRH. Solar systems and their integration with heat pumps: a review. Energy Buildings 2015;87:395–412.
- [17] Buker MS, Riffat SB. Solar assisted heat pump systems for low temperature water heating applications: a systematic review. Renew Sustain Energy Rev 2016;55: 399–413.

- [18] Wang ZY, Guo P, Zhang HJ, Yang WS, Mei S. Comprehensive review on the development of SAHP for domestic hot water. Renew Sustain Energy Rev 2017; 72:871–81.
- [19] Poppi S, Sommerfeldt N, Bales C, Madani H, Lundqvist P. Techno-economic review of solar heat pump systems for residential heating applications. Renew Sustain Energy Rev 2018;81:22–32.
- [20] Mohanraj M, Ye B, Jayaraj S, Kaltayev A. Research and developments on solar assisted compression heat pump systems – A comprehensive review (Part A: modeling and modifications). Renew Sustain Energy Rev 2018;83:90–123.
- [21] Mohanraj M, Ye B, Jayaraj S, Kaltayev A. Research and developments on solar assisted compression heat pump systems a comprehensive review (Part-B: applications). Renew Sustain Energy Rev 2018;83:124–55.
- [22] Wang XR, Xia L, Bales C, Zhang XX, Copertaro B, Pan S, et al. A systematic review of recent air source heat pump (ASHP) systems assisted by solar thermal, photovoltaic and photovoltaic/thermal sources. Renew Energy 2020;146: 2472–87
- [23] Sezen K, Tuncer AD, Akyuz AO, Gungor A. Effects of ambient conditions on solar assisted heat pump systems: a review. Sci Total Environ 2021;778:146362.
- [24] Abou-Ziyan HZ, Ahmed MF, Metwally MN, Abd E-H. Solar-assisted R22 and R134a heat pump systems for low-temperature applications. Appl Therm Eng 1997;17:455–69.
- [25] Karagiorgas M, Galatis K, Tsagouri M, Tsoutsos T, Botzios-Valaskakis A. Solar assisted heat pump on air collectors: a simulation tool. Sol Energy 2010;84: 66–78.
- [26] Asaee SR, Ugursal VI, Beausoleil-Morrison I. Techno-economic assessment of solar assisted heat pump system retrofit in the Canadian housing stock. Appl Energy 2017;190:439–52.
- [27] International Energy Agency. Technology road map solar heating and cooling. 2012. http://www.iea-shc.org/data/sites/1/publications/2012_SolarHeatingCooling_Roadmap.pdf. [accessed 10 September 2020].
- [28] Carbonell D, Haller MY, Frank E. Potential benefit of combining heat pumps with solar thermal for heating and domestic hot water preparation. Energy Procedia 2014;57:2656–65.
- [29] Cai JY, Li ZH, Ji J, Zhou F. Performance analysis of a novel air source hybrid solar assisted heat pump. Renew Energy 2019;139:1133–45.
- [30] Hesaraki A, Holmberg S, Haghighat F. Seasonal thermal energy storage with heat pumps and low temperatures in building projects - a comparative review. Renew Sustain Energy Rev 2015;43:1199–213.
- [31] Kaygusuz K. Investigation of a combined solar-heat pump system for residential heating. Part 2: simulation results. Int J Energy Res 1999;23:1225–37.
- [32] Chow TT, Pei G, Fong KF, Lin Z, Chan ALS, He M. Modelling and application of direct-expansion solar-assisted heat pump for water heating in subtropical Hong Kong. Appl Energy 2010;87:643–9.
- [33] Chaturvedi SK, Shen JY. Thermal performance of a direct expansion solar-assisted heat pump. Sol Energy 1984;33:155–62.
- [34] Deng W, Yu J. Simulation analysis on dynamic performance of a combined solar/ air dual source heat pump water heater. Energy Convers Manage 2016;120: 378–87.
- [35] Huang BJ, Lee JP, Chyng JP. Heat-pipe enhanced solar-assisted heat pump water heater. Sol Energy 2005;78:375–81.
- [36] Chaturvedi SK, Abdel-Salam TM, Sreedharan SS, Gorozabel FB. Two-stage direct expansion solar-assisted heat pump for high temperature applications. Appl Therm Eng 2005;29:2093–9.
- [37] Kuang YH, Wang RZ. Performance of a multi-functional direct-expansion solar assisted heat pump system. Sol Energy 2006;80:795–803.
- [38] Zhu L, Yu JL, Zhou ML, Wang X. Performance analysis of a novel dual-nozzle ejector enhanced cycle for solar assisted air-source heat pump systems. Renew Energy 2014;63:735–40.
- [39] Yan G, Bai T, Yu J. Energy and exergy efficiency analysis of solar driven ejector—compressor heat pump cycle. Sol Energy 2016;125:243–55.
- [40] Chen J, Yu J. Theoretical analysis on a new direct expansion solar assisted ejector-compression heat pump cycle for water heater. Sol Energy 2017;142: 299–307
- [41] Bakirci K, Yuksel B. Experimental thermal performance of a solar source heatpump system for residential heating in cold climate region. Appl Therm Eng 2011;31:1508–18.
- [42] Yumrutas R, Kaska O. Experimental investigation of thermal performance of a solar assisted heat pump system with an energy storage. Int J Energy Res 2004; 28:163–75.
- [43] Li H, Yang HX. Study on performance of solar assisted air source heat pump systems for hot water production in Hong Kong. Appl Energy 2010;87:2818–25.
- [44] Cai JY, Ji J, Wang YY, Huang WZ. Numerical simulation and experimental validation of indirect expansion solar-assisted multi-functional heat pump. Renew Energy 2016;93:280–90.
- [45] Air-Conditioning, Heating, and Refrigeration Institute. 2008 standard for performance rating of unitary air-conditioning & air-source heat pump equipment. 2012. http://www.ahrinet.org/App_Content/ahri/files/standards% 20pdfs/ANSI%20standards%20pdfs/ANSI.AHRI%20Standard%20210.240%20 with%20Addenda%201%20and%202.pdf. [accessed 11 September 2020].
- [46] Lerch W, Heinz A, Heimrath R. Direct use of solar energy as heat source for a heat pump in comparison to a conventional parallel solar air heat pump system. Energy Buildings 2015;100:34–42.
- [47] Kaygusuz K. Experimental and theoretical investigation of a solar heating system with heat pump. Renew Energy 2000;21:79–102.
- [48] Kaygusuz K. Investigation of a combined solar-heat pump system for residential heating. Part 1: experimental results. Int J Energy Res 1999;23:1213–23.

- [49] Dikici A, Akbulut A. Exergetic performance evaluation of heat pump systems having various heat sources. Int J Energy Res 2008;32:1279–96.
- [50] Liu Y, Ma J, Zhou GH, Zhang C, Wan WL. Performance of a solar air composite heat source heat pump system. Renew Energy 2016;87:1053–8.
- [51] Yerdesh Y, Abdulina Z, Aliuly A, Belyayev Y, Mohanraj M, Kaltayev A. Numerical simulation on solar collector and cascade heat pump combi water heating systems in Kazakhstan climates. Renew Energy 2020;145:1222–34.
- [52] Lv XL, Yan G, Yu JL. Solar-assisted auto-cascade heat pump cycle with zeotropic mixture R32/R290 for small water heaters. Renew Energy 2015;76:167–72.
- [53] Sterling SJ. Feasibility analysis of two indirect heat pump assisted solar domestic hot water systems. M.S. thesis. Canada: University of Waterloo; 2011.
- [54] Sterling SJ, Collins MR. Feasibility analysis of an indirect heat pump assisted solar domestic hot water system. Appl Energy 2012;93:11–7.
- [55] Deng S, Dai YJ, Wang RZ. Performance study on hybrid solar-assisted CO2 heat pump system based on the energy balance of net zero energy apartment. Energy Buildings 2012;54:337–49.
- [56] Faria RN, Nunes RO, Koury RNN, Machado L. Dynamic modeling study for a solar evaporator with expansion valve assembly of a transcritical CO₂ heat pump. Int J Refrig 2016;64:203–13.
- [57] Deng S, Dai YJ, Wang RZ. Performance optimization and analysis of solar combisystem with carbon dioxide heat pump. Sol Energy 2013;98:212–25.
- [58] Chen JF, Dai YJ, Wang RZ. Experimental and theoretical study on a solar assisted CO₂ heat pump for space heating. Renew Energy 2016;89:295–304.
- [59] Ziemelis I, Kancevica L, Jesko Z, Putans H. Calculation of energy produced by solar collectors. In: Proceedings of Engineering for Rural Development: Jelgava, Latvia; 2009.
- [60] Sun XL, Dai YJ, Novakovic V, Wu J, Wang RZ. Performance comparison of direct expansion solar-assisted heat pump and conventional air source heat pump for domestic hot water. Energy Procedia 2015;70:394–401.
- [61] Scarpa F, Tagliafico LA. Exploitation of humid air latent heat by means of solar assisted heat pumps operating below the dew point. Appl Therm Eng 2016;100: 820–8.
- [62] Trinkl C, Zörner W, Hanby V. Simulation study on a domestic solar/heat pump heating system incorporating latent and stratified thermal storage. J Solar Energy Eng 2009;131:041008.
- [63] Freeman TL, Mitchell JW, Audit TE. Performance of combined solar-heat pump systems. Sol Energy 1979;22:125–35.
- [64] Kaygusuz K, Comakli O, Ayhan T. Solar-assisted heat pump systems and energy storage. Sol Energy 1991;47:383–91.
- [65] Chyng JP, Lee CP, Huang BJ. Performance analysis of a solar-assisted heat pump water heater. Sol Energy 2003;74:33–44.
- [66] Kaygusuz K. Calculation of required collector area of a solar-assisted series heat pump for domestic heating. Energy Sources 2000;22:247–56.
- [67] Kuang YH, Wang RZ, Yu LQ. Experimental study on solar assisted heat pump system for heat supply. Energy Convers Manage 2003;44:1089–98.
- [68] Yumrutas R, Unsal M. Analysis of solar aided heat pump systems with seasonal thermal energy storage in surface tanks. Energy 2000;25:1231–43.
- [69] Yumrutas R, Kunduz M, Ayhan T. Investigation of thermal performance of a ground coupled heat pump system with a cylindrical energy storage tank. Int J Energy Res 2003;27:1051–66.
- [70] Kuang YH, Sumathy K, Wang RZ. Study on a direct-expansion solar-assisted heat pump water heating system. Int J Energy Res 2003;27:531–48.
- [71] Xu GY, Zhang XS, Deng SM. A simulation study on the operating performance of a solar–air source heat pump water heater. Appl Therm Eng 2006;26:1257–65.
- [72] Li YW, Wang RZ, Wu JY, Xu YX. Experimental performance analysis and optimization of a direct expansion solar-assisted heat pump water heater. Energy 2007;32:1361–74.
- [73] Kong XQ, Zhang D, Li Y, Yang QM. Thermal performance analysis of a direct-expansion solar-assisted heat pump water heater. Energy 2011;36:6830–8.
- [74] Li YW, Wang RZ, Wu JY, Xu YX. Experimental performance analysis on a directexpansion solar-assisted heat pump water heater. Appl Therm Eng 2007;27: 2858–68.
- [75] Dikici A, Akbulut A. Performance characteristics and energy-exergy analysis of solar-assisted heat pump system. Building Environ 2008;43:1961–72.
- [76] Ito S, Miura N, Wang K. Performance of a heat pump using direct expansion solar collectors. Sol Energy 1999;65:189–96.
- [77] Dong X, Tian Q, Li Z. Energy and exergy analysis of solar integrated air source heat pump for radiant floor heating without water. Energy Buildings 2017;142: 128–38.
- [78] Caglar A, Yamalı C. Performance analysis of a solar-assisted heat pump with an evacuated tubular collector for domestic heating. Energy Buildings 2012;54:22–8.
- [79] Liang CH, Zhang XS, Li XW, Zhu X. Study on the performance of a solar assisted air source heat pump system for building heating. Energy Buildings 2011;43: 2188–96.
- [80] Qu SL, Ma F, Ji R, Wang DX, Yang LX. System design and energy performance of a solar heat pump heating system with dual-tank latent heat storage. Energy Buildings 2015;105:294–301.
- [81] Youssef W, Ge YT, Tassou SA. Effects of latent heat storage and controls on stability and performance of a solar assisted heat pump system for domestic hot water production. Sol Energy 2017;150:394–407.
- [82] Carbonell D, Haller MY, Philippen D, Frank E. Simulations of combined solar thermal and heat pump systems for domestic hot water and space heating. Energy Procedia 2014;48:524–34.
- [83] Ortiz-Rivera EI, Feliciano-Cruz LI. Performance evaluation and simulation of a solar thermal power plant. In: Proceedings of the IEEE energy conversion congress and exposition. San Jose, California, USA. 2009.

- [84] Eslami-nejad P, Bernier M. Coupling of geothermal heat pumps with thermal solar collectors using double U-tube boreholes with two independent circuits. Appl Therm Eng 2011;31:3066–77.
- [85] Wang QK, Huang Q. Research on integrated solar and geothermal energy engineering design in hot summer and cold winter area. Procedia Eng 2011;21: 648–55.
- [86] Cristofari C, Notton G, Poggi P, Louche A. Influence of the flow rate and the tank stratification degree on the performances of a solar flat-plate collector. Int J Therm Sci 2003;42:455–69.
- [87] Han YM, Wang RZ, Dai YJ. Thermal stratification within the water tank. Renew Sustain Energy Rev 2009;13:1014–26.
- [88] Ghaddar NK. Stratified storage tank influence on performance of solar water heating system tested in Beirut. Renew Energy 1994;4:911–25.
- [89] Huang HL, Ge XS, Su YH. Theoretical thermal performance analysis of two solar-assisted heat-pump systems. Int J Energy Res 1999;23:1–6.
- [90] Carbonell D, Philippen D, Granzotto M, Haller MY, Frank E. Simulation of combined solar thermal, heat pump, ice storage and waste water heat recovery systems. Design Criteria and Parametric Studies. Proceedings of EuroSun ISES, Aixlse Bains, France. 2014.
- [91] Han ZW, Zheng MY, Kong FH, Wang F, Li ZJ, Bai T. Numerical simulation of solar assisted ground-source heat pump heating system with latent heat energy storage in severely cold area. Appl Therm Eng 2008;28:1427–36.
- [92] Zivkovic B, Fujii I. An analysis of isothermal phase change of phase change material within rectangular and cylindrical containers. Sol Energy 2001;70: 51, 61
- [93] Niu FX, Ni L, Qu ML, Yao Y, Deng SM. A novel triple-sleeve energy storage exchanger and its application in an environmental control system. Appl Therm Eng 2013:54:1-6.
- [94] Ni L, Qv DH, Yao Y, Niu FX, Hu WJ. An experimental study on performance enhancement of a PCM based solar-assisted air source heat pump system under cooling modes. Appl Therm Eng 2016;100:434–52.
- [95] Qv DH, Ni L, Yao Y, Hu WJ. Reliability verification of a solar-air source heat pump system with PCM energy storage in operating strategy transition. Renew Energy 2015;84:46–55.
- [96] Kaygusuz K. Utilization of solar energy and waste heat. Energy Sources 1999;21: 595–610.
- [97] Tamasauskas J, Poirier M, Zmeureanu R, Kegel M, Sunye R. Development and validation of a solar-assisted heat pump using ice slurry as a latent storage material. Sci Tech Built Environ 2015;21:837–46.
- [98] Carbonell D, Philippen D, Haller MY, Frank E. Development and validation of a mathematical model for ice storages with heat exchangers that can be de-iced. Energy Procedia 2014;57:2342–51.
- [99] Carbonell D, Philippen D, Haller MY, Frank E. Modeling of an ice storage based on a de-icing concept for solar heating applications. Sol Energy 2015;121:2–16.
- [100] Carbonell D, Philippen D, Haller MY, Brunold S. Modeling of an ice storage buried in the ground for solar heating applications. Validations with one year of monitored data from a pilot plant. Sol Energy 2016;125:398–414.
- [101] Esen M. Thermal performance of a solar-aided latent heat store used for space heating by heat pump. Sol Energy 2000;69:15–25.
- [102] Schmidt T, Mangold D, Muller-Steinhagen H. Central solar heating plants with seasonal storage in Germany. Sol Energy 2004;76:165–74.
- [103] Gao LH, Zhao J, Tang ZP. A review on borehole seasonal solar thermal energy storage. Energy Procedia 2015;70:209–18.
- [104] Reuss M, Beuth W, Schmidt M, Schoelkopf W. Solar district heating with seasonal storage in Attenkirchen. In: Proceedings of the IEA Conf ECOSTOCK. New Jersey, USA. 2006.
- [105] Hasnain SM. Review on sustainable thermal energy storage technologies, part i: heat storage materials and techniques. Energy Convers Manage 1998;39: 1127–38.
- [106] Shah SK, Aye L, Rismanchi B. Seasonal thermal energy storage system for cold climate zones: a review of recent developments. Renew Sustain Energy Rev 2018; 97:38–49.
- [107] Gari HN, Loehrke RI. A controlled buoyant jet for enhancing stratification in a liquid storage tank. J Fluids Eng 1982;104:475–81.
- [108] Xu RJ, Zhao YQ, Chen H, Wu Q, Yang LW, Wang HS. Numerical and experimental investigation of a compound parabolic concentrator-capillary tube solar collector. Energy Convers Manage 2020;204:112218.
- [109] Qi Q, Deng SM, Jiang YQ. A simulation study on a solar heat pump heating system with seasonal latent heat storage. Sol Energy 2008;82:669–75.
- [110] Yao Y, Jiang YQ, Deng SM, Ma ZL. A study on the performance of the airside heat exchanger under frosting in an air source heat pump water heater/chiller unit. Int J Heat Mass Transfer 2004;47:3745–56.
- [111] Kondepudi S, O'Neal DL. Frosting performance of tube fin heat exchangers with wavy and corrugated fins. Exp Therm Fluid Sci 1991;4:613–8.
- [112] Sheng W, Liu PP, Dang CB, Liu GX. Review of restraint frost method on cold surface. Renew Sustain Energy Rev 2017;79:806–13.
- [113] Kim MH, Kim H, Lee KS, Kim DR. Frosting characteristics on hydrophobic and superhydrophobic surfaces: a review. Energy Convers Manage 2017;138:1–11.
- [114] Song MJ, Deng SM, Dang CB, Mao N, Wang ZH. Review on improvement for air source heat pump units during frosting and defrosting. Appl Energy 2018;211: 1150–70.
- [115] Byun JS, Jeon CD, Jung JH, Lee JH. The application of photo-coupler for frost detecting in an air-source heat pump. Int J Refrig 2006;29:191–8.
- [116] Jang JY, Bae HH, Lee SJ, Ha MY. Continuous heating of an air-source heat pump during defrosting and improvement of energy efficiency. Appl Energy 2013;110: 9–16.

- [117] Tang JC, Gong GC, Su H, Wu FH, Herman C. Performance evaluation of a novel method of frost prevention and retardation for air source heat pumps using the orthogonal experiment design method. Appl Energy 2016;169:696–708.
- [118] Jiang YQ, Fu HY, Yao Y, Yan L, Gao Q. Experimental study on concentration change of spray solution used for a novel non-frosting air source heat pump system. Energy Buildings 2014;68:707–12.
- [119] Wu XM, Webb RL. Investigation of the possibility of frost release from a cold surface. Exp Therm Fluid Sci 2001;24:151–6.
- [120] Shen JB, Qian ZJ, Xing ZW, Yu Y, Ge MC. A review of the defrosting methods of air source heat pumps using heat exchanger with phase change material. Energy Procedia 2019;160:491–8.
- [121] Qu ML, Xia L, Deng SM, Jiang YQ. Improved indoor thermal comfort during defrost with a novel reverse-cycle defrosting method for air source heat pumps. Building Environ 2010;45:2354–61.
- [122] Hu WJ, Jiang YQ, Qu ML, Ni L, Yao Y, Deng SM. An experimental study on the operating performance of a novel reverse-cycle hot gas defrosting method for air source heat pumps. Appl Therm Eng 2011;31:363–9.
- [123] Zhang L, Dong J, Jiang YQ, Yao Y. A novel defrosting method using heat energy dissipated by the compressor of an air source heat pump. Appl Energy 2014;133: 101–11
- [124] Wang ZH, Zheng YX, Wang FH, Wang XK, Lin Z, Li JC, et al. Experimental analysis on a novel frost-free air-source heat pump water heater system. Appl Therm Eng 2014:70:808–16.
- [125] Wang FH, Wang ZH, Zheng YX, Lin Z, Hao PF, Huan Ch, et al. Performance investigation of a novel frost-free air-source heat pump water heater combined with energy storage and dehumidification. Appl Energy 2015;139:212–9.
- [126] Mohamed E, Riffat S, Omer S. Low-temperature solar-plate-assisted heat pump: A developed design for domestic applications in cold climate. Int J Refrig 2017;81:
- [127] Kong XQ, Li JY, Wang BG, Li Y. Numerical study of a direct-expansion solarassisted heat pump water heater under frosting conditions based on experiments. Solar Energy 2020;196:10-2.
- [128] Huang WZ, Ji J, Xu N, Li GQ. Frosting characteristics and heating performance of a direct-expansion solar-assisted heat pump for space heating under frosting conditions. Appl Energy 2016;171:656–66.
- [129] James A, Mohanraj M, Srinivas M, Jayaraj S. Thermal analysis of heat pump systems using photovoltaic-thermal collectors: a review. J Therm Anal Calorim 2021;144:1–39.
- [130] Breidenich C, Magraw D, Rowley A, Rubin J. The Kyoto protocol to the United Nations framework convention on climate change. American J Int Law 1998;92: 315–31.
- [131] Heath E. Amendment to the Montreal protocol on substances that deplete the ozone layer (Kigali Amendment). Int Legal Materials 2017;56:193–205.
- [132] United Nations Environment Programme. The Montreal protocol on substances that deplete the ozone layer. 1987. https://unep.ch/ozone/pdf/Montreal-Protoco 12000.pdf. [accessed 10 September 2020].
- [133] International Electrotechnical Commission. https://webstore.iec.ch/publication/ 62243. [accessed 25 October 2020].
- [134] Chaturvedi SK, Chen DT, Kheireddine A. Thermal performance of a variable capacity direct expansion solar-assisted heat pump. Energy Convers Manage 1998;39:181–91.
- [135] Paradeshia L, Srinivasb M, Jayaraj S. Parametric studies of a simple direct expansion solar assisted heat pump operating in a hot and humid environment. Energy Procedia 2016;90:635–44.
- [136] Molinaroli L, Joppolo CM, De Antonellis S. Numerical analysis of the use of R-407C in direct expansion solar assisted heat pump. Energy Procedia 2014;48: 938–45.
- [137] Huang BJ, Chyng JP. Performance characteristics of integral type solar-assisted heat pump. Sol Energy 2001;71:403–14.
- [138] Anderson TN, Morrison GL. Effect of load pattern on solar-boosted heat pump water heater performance. Sol Energy 2007;81:1386–95.
- [139] Mohanraj M, Jayaraj S, Muraleedharan C. Modeling of a direct expansion solar assisted heat pump using artificial neural networks. Int J Green Energy 2008;5: 520–32.
- [140] Axaopoulos P, Panagakis P, Kyritsis S. Experimental comparison of a solarassisted heat pump vs. a conventional thermosyphon solar system. Int J Energy Res 1998;22:1107–20.
- [141] Huang BJ, Lee CP. Long-term performance of solar-assisted heat pump water heater. Renew Energy 2003;29:633–9.
- [142] Huang BJ, Lee CP. Performance evaluation method of solar-assisted heat pump water heater. Appl Therm Eng 2007;27:568–75.
- [143] Moreno-Rodríguez A, González-Gil A, Izquierdo M, Garcia-Hernando N. Theoretical model and experimental validation of a direct-expansion solar assisted heat pump for domestic hot water applications. Energy 2012;45:704–15.
- [144] Moreno-Rodríguez A, Garcia-Hernando N, González-Gil A, Izquierdo M. Experimental validation of a theoretical model for a direct-expansion solarassisted heat pump applied to heating. Energy 2013;60:242–53.
- [145] Mohanraj M, Jayaraj S, Muraleedharan C. Performance prediction of a direct expansion solar assisted heat pump using artificial neural networks. Appl Energy 2009;86:1442–9.
- [146] Ito S, Miura N, Takano Y. Studies of heat pumps using direct expansion type solar collectors. J Solar Energy Eng 2005;127:60–4.
- [147] Mohanraj M, Jayaraj S, Muraleedharan C. Exergy analysis of direct expansion solar-assisted heat pumps using artificial neural networks. Int J Energy Res 2009; 33:1005–20.

- [148] Huang BJ, Chyng JP. Integral-type solar-assisted heat pump water heater. Renew Energy 1999;16:731–4.
- [149] Sun XL, Wu JY, Dai YJ, Wang RZ. Experimental study on roll-bond collector/ evaporator with optimized channel used in direct expansion solar assisted heat pump water heating system. Appl Therm Eng 2014;66:571–9.
- [150] Fernández-Seara J, Piñeiro C, Alberto DJ, Fernandes F, Sousa PXB. Experimental analysis of a direct expansion solar assisted heat pump with integral storage tank for domestic water heating under zero solar radiation conditions. Energy Convers Manage 2012;59:1–8.
- [151] Gorozabel CFB, Chaturvedi SK, Almogbel A. Analysis of a direct expansion solar assisted heat pump using different refrigerants. Energy Convers Manage 2005;46: 2614–24
- [152] Aziz W, Chaturvedi SK, Kheireddine A. Thermodynamic analysis of two-component, two-phase flow in solar collectors with application to a direct-expansion solar-assisted heat pump. Energy 1999;24:247–59.
- [153] Chaturvedi SK, Gagrani VD, Abdel-Salam TM. Solar-assisted heat pump A sustainable system for low-temperature water heating applications. Energy Convers Manage 2014;77:550–7.
- [154] Zhang D, Wu QB, Li JP, Kong XQ. Effects of refrigerant charge and structural parameters on the performance of a direct-expansion solar-assisted heat pump system. Appl Therm Eng 2014;73:522–8.
- [155] Scarpa F, Tagliafico LA, Tagliafico G. Integrated solar-assisted heat pumps for water heating coupled to gas burners; control criteria for dynamic operation. Appl Therm Eng 2011;31:59–68.
- [156] Tagliafico LA, Scarpa F, Valsuani F. Direct expansion solar assisted heat pumps: a clean steady state approach for overall performance analysis. Appl Therm Eng 2014:66:216–26.
- [157] Kong XQ, Li Y, Lin L, Yang YG. Modeling evaluation of a direct-expansion solar assisted heat pump water heater using R410A. Int J Refrig 2017;76:136–46.
- [158] Scarpa F, Tagliafico LA, Bianco V. A novel steady-state approach for the analysis of gas-burner supplemented direct expansion solar assisted heat pumps. Sol Energy 2013;96:227–38.
- [159] Chaturvedi SK, Mohieldin TO, Chen DT. Second-law analysis of solar-assisted heat pumps. Energy 1991;16:941–9.
- [160] Aye L, Charters WWS, Chaichana C. Solar heat pump systems for domestic hot water. Sol Energy 2002;73:169–75.
- [161] Li H, Yang HX. Potential application of solar thermal systems for hot water production in Hong Kong. Appl Energy 2009;86:175–80.
- [162] Torres-Reyes E, Cervantes JG. Optimal performance of an irreversible solarassisted heat pump. Exergy, an Int J 2001;1:107–11.
- [163] Torres-Reyes E, Picon-Nunez M, Cervantes JG. Exergy analysis and optimization of a solar-assisted heat pump. Energy 1998;23:337–44.
- [164] Cervantes JG, Torres-Reyes E. Experiments on a solar-assisted heat pump and an exergy analysis of the system. Appl Therm Eng 2002;22:1289–97.
- [165] Chow TT, Bai Y, Fong KF, Lin Z. Analysis of a solar assisted heat pump system for indoor swimming pool water and space heating. Appl Energy 2012;100:309–17.
- [166] Chaichana C, Kiatsiriroat T, Nuntaphan A. Comparison of conventional flat-plate solar collector and solar boosted heat pump using unglazed collector for hot water production in small slaughterhouse. Heat Transfer Eng 2010;31:419–29.
- [167] Fraga C, Mermoud F, Hollmuller P, Pampaloni E, Lachal B. Large solar driven heat pump system for a multifamily building: long term in-situ monitoring. Sol Energy 2015:114:427–39.
- [168] Nuntaphan A, Chansena C, Kiatsiriroat T. Performance analysis of solar water heater combined with heat pump using refrigerant mixture. Appl Energy 2009;86: 748–56
- [169] Banister CJ, Collins MR. Development and performance of a dual tank solarassisted heat pump system. Appl Energy 2015;149:125–32.
- assisted heat pump system. Appl Energy 2015;149:125–32.
 [170] He W, Hong XQ, Zhao XD, Zhang XX, Shen JC, Ji J. Operational performance of a novel heat pump assisted solar façade loop-heat-pipe water heating system. Appl Energy 2015;146:371–82.
- [171] Wang Q, Ren B, Zeng ZY, He W, Liu YQ, Xu XG, et al. Development of a novel indirect-expansion solar-assisted multifunctional heat pump with four heat exchangers. Building Services Eng Res Tech 2015;36:469–81.
- [172] Wang Q, Liu YQ, Liang GF, Li JR, Sun SF, Chen GM. Development and experimental validation of a novel indirect-expansion solar-assisted multifunctional heat pump. Energy Buildings 2011;43:300–4.
- [173] Winteler C, Dott R, Afjei T, Hafner B. Seasonal performance of a combined solar, heat pump and latent heat storage system. Energy Procedia 2014;48:689–700.
- [174] Tamasauskas J, Poirier M, Zmeureanu R, Sunye R. Modeling and optimization of a solar assisted heat pump using ice slurry as a latent storage material. Sol Energy 2012;86:3316–25.
- [175] Li H, Sun LL, Zhang YG. Performance investigation of a combined solar thermal heat pump heating system. Appl Therm Eng 2014;71:460–8.
- [176] Bellos E, Tzivanidis C. Energetic and financial sustainability of solar assisted heat pump heating systems in Europe. Sustain Cities Society 2017;33:70–84.
- [177] He W, Hong XQ, Zhao XD, Zhang XX, Shen JC, Ji J. Theoretical investigation of the thermal performance of a novel solar loop-heat-pipe facade-based heat pump water heating system. Energy Buildings 2014;77:180–91.
- [178] Tagliafico LA, Scarpa F, Tagliafico G, Valsuani F. An approach to energy saving assessment of solar assisted heat pumps for swimming pool water heating. Energy Buildings 2012;55:833–40.
- [179] Li QY, Chen Q, Zhang X. Performance analysis of a rooftop wind solar hybrid heat pump system for buildings. Energy Buildings 2013;65:75–83.
- [180] Panaras G, Mathioulakis E, Belessiotis V. Investigation of the performance of a combined solar thermal heat pump hot water system. Sol Energy 2013;93: 169–82.

- [181] Shan M, Yu T, Yang X. Assessment of an integrated active solar and air-source heat pump water heating system operated within a passive house in a cold climate zone. Renew Energy 2016;87:1059–66.
- [182] Li YH, Kao WC. Performance analysis and economic assessment of solar thermal and heat pump combisystems for subtropical and tropical region. Sol Energy 2017;153:301–16.
- [183] Panaras G, Mathioulakis E, Belessiotis V. A method for the dynamic testing and evaluation of the performance of combined solar thermal heat pump hot water systems. Appl Energy 2014;114:124–34.
- [184] Poppi S, Bales C, Haller MY, Heinz A. Influence of boundary conditions and component size on electricity demand in solar thermal and heat pump combisystems. Appl Energy 2016;162:1062–73.
- [185] Poppi S, Bales C, Heinz A, Hengel F, Chèze D, Mojic I, et al. Analysis of system improvements in solar thermal and air source heat pump combi systems. Appl Energy 2016:173:606–23.
- [186] Ji J, Cai JY, Huang WZ, Feng Y. Experimental study on the performance of solar-assisted multi-functional heat pump based on enthalpy difference lab with solar simulator. Renew Energy 2015;75:381–8.
- [187] Ni L, Qv DH, Shang RX, Yao Y, Niu FX, Hu WJ. Experimental study on performance of a solar-air source heat pump system in severe external conditions and switchover of different functions. Sustain Energy Tech Assess 2016;16: 162–73.
- [188] Xu RJ, Hu WJ, Wu QP, Wang RX, Wang HS, Hu J. Liquid flow control method for heating plant and thermal energy collector. ZL201610792318.7. Issued date 18th June 2019
- [189] International Energy Agency. Solar heat worldwide–global market development and trends in 2019 & detailed market data 2018. https://www.iea-shc. org/solar-heat-worldwide-2020. [accessed 10 September 2020].
- [190] Li YH. Variable frequency drive applications in HVAC systems. IntechOpen: New Applications of Electric Drives. Miroslav Chomat; 2015.
- [191] Lerch W, Heinz A, Heimrath R. Evaluation of combined solar thermal heat pump systems using dynamic system simulations. Energy Procedia 2014;48:598–607.
- [192] Hawlader MNA, Chou SK, Ullah MZ. The performance of a solar assisted heat pump water heating system. Appl Therm Eng 2001;21:1049–65.
- [193] Kong XQ, Sun PL, Jiang KL, Dong SD, Li Y, Li JB. A variable frequency control method and experiments of a direct-expansion solar-assisted heat pump system. Sol Energy 2018;176:572–80.
- [194] Kong XQ, Wang BG, Shang YP, Li JY, Li Y. Influence of different regulation modes of compressor speed on the performance of direct-expansion solar-assisted heat pump water heater. Appl Therm Eng 2020;169:115007.
- [195] Kong XQ, Zhang MY, Yang YM, Li Y, Wang DC. Comparative experimental analysis of direct-expansion solar-assisted heat pump water heaters using R134a and R290. Sol Energy 2020;203:187–96.
- [196] Kong XQ, Sun PL, Dong SD, Jiang KL, Li Y. Experimental performance analysis of a direct-expansion solar-assisted heat pump water heater with R134a in summer. Int J Refrig 2018;91:12–9.
- [197] Kong XQ, Yang YM, Zhang MY, Li Y, Li JB. Experimental investigation on a direct-expansion solar-assisted heat pump water heater using R290 with micro-channel heat transfer technology during the winter period. Int J Refrig 2020;113:38–48.
- [198] Kong XQ, Jiang KL, Dong SD, Li Y, Li JB. Control strategy and experimental analysis of a direct-expansion solar-assisted heat pump water heater with R134a. Energy 2018;145:17–24.
- [199] Kong XQ, Sun PL, Li Y, Jiang KL, Dong SD. Experimental studies of a variable capacity direct-expansion solar-assisted heat pump water heater in autumn and winter conditions. Sol Energy 2018;170:352–7.
- [200] Dong X, Tian Q, Li Z. Experimental investigation on heating performance of solar integrated air source heat pump. Appl Therm Eng 2017;123:1013–20.
- [201] Xian T, Wu JH, Zhang X. Study on the operating characteristics of a solar heat pump water heater based on data fusion. Sol Energy 2020;212:113–24.
- [202] Wu JH, Xian T, Liu X. All-weather characteristic studies of a direct expansion solar integrated air source heat pump system based on PCMs. Sol Energy 2019; 191:34–45.
- [203] Kutlu C, Zhang YN, Elmer T, Su YH, Riffat S. A simulation study on performance improvement of solar assisted heat pump hot water system by novel controllable crystallization of supercooled PCMs. Renew Energy 2020;152:601–12.
- [204] Buker SM, Riffat SB. Build-up and performance test of a novel solar thermal roof for heat pump operation. Int J Ambient Energy 2017;38:365–79.
- [205] Huan C, Wang FH, Li ST, Zhao YJ, Liu L, Wang ZH, et al. A performance comparison of serial and parallel solar-assisted heat pump heating systems in Xi'an. China. Energy Sci Eng 2019;7:1379–93.
- [206] Liu FZ, Wang L, Wang Q, Wang HF. Experiment study on heating performance of solar-air source heat pump unit. Procedia Eng 2017;205:3873–8.
- [207] Ran SY, Lyu WH, Li XT, Xu W, Wang BL. A solar-air source heat pump with thermosiphon to efficiently utilize solar energy. J Building Eng 2020;31:101330.
- [208] Liu ZJ, Liu YW, Wu D, Jin GY, Yu HC, Ma WS. Performance and feasibility study of solar-air source pump systems for low-energy residential buildings in Alpine regions. J Cleaner Prod 2020;256:120735.
- [209] Kim T, Choi BI, Han YS, Do KH. A comparative investigation of solar-assisted heat pumps with solar thermal collectors for a hot water supply system. Energy Convers Manage 2018;172:472–84.
- [210] Qiu GD, Wei XH, Xu ZF, Cai WH. A novel integrated heating system of solar energy and air source heat pumps and its optimal working condition range in cold regions. Energy Convers Manage 2018;174:922–31.
- [211] Long JB, Xia KM, Zhong HH, Lu HL, A YG. Study on energy-saving operation of a combined heating system of solar hot water and air source heat pump. Energy Convers Manage 2021;220:113624.

- [212] Chargui R, Awani S. Determining of the optimal design of a closed loop solar dual source heat pump system coupled with a residential building application. Energy Convers Manage 2017;147:40–54.
- [213] Huang WZ, Zhang T, Ji J, Xu N. Numerical study and experimental validation of a direct-expansion solar-assisted heat pump for space heating under frosting conditions. Energy Building 2019;185:224–38.
- [214] Cai JY, Ji J, Wang YY, Huang WZ. Operation characteristics of a novel dual source multi-functional heat pump system under various working modes. Appl Energy 2017;194:236–46.
- [215] Cai JY, Zhang F, Ji J. Comparative analysis of solar-air dual source heat pump system with different heat source configurations. Renew Energy 2020;150: 101 203
- [216] Zhang F, Cai JY, Ji J, Han KD, Ke W. Experimental investigation on the heating and cooling performance of a solar air composite heat source heat pump. Renew Energy 2020:161:221–9.
- [217] Ji WA, Cai JY, Ji J, Huang WZ. Experimental study of a direct expansion solarassisted heat pump (DX-SAHP) with finned-tube evaporator and comparison with conventional DX-SAHP. Energy Buildings 2020;207:109632.
- [218] Rabelo SN, Paulino TF, Duarte WM, Sawalha W, Machado L. Experimental analysis of the influence of water mass flow rate on the performance of a CO₂ direct-expansion solar assisted heat pump. Int Scho Sci Res Innov 2018;12:
- [219] Treichel C, Cruickshank CA. Energy analysis of heat pump water heaters coupled with air-based solar thermal collectors in Canada and the United States. Energy 2021;221:119801.
- [220] Treichel C, Cruickshank CA. Greenhouse gas emissions analysis of heat pump water heaters coupled with air-based solar thermal collectors in Canada and the United States. Energy Buildings 2021;231:110594.
- [221] Treichel C, Cruickshank CA. Analysis of a coupled air-based solar collector and heat pump water heater in Canada and the United States. IEA SHC Int Conf on Solar Heating and Cooling for Buildings and Industry. 2019.
- [222] Li YL, Li BG, Liu CY, Su SQ, Xiao HH, Zhu CH. Design and experimental investigation of a phase change energy storage air-type solar heat pump heating system. Appl Therm Eng 2020;179:115506.
- [223] Aktas M, Kosan M, Arslan E, Tuncer AD. Designing a novel solar-assisted heat pump system with modification of a thermal energy storage unit. J Power Energy 2019;233:588–603.
- [224] Kaygusuz K. Performance of solar assisted parallel and series heat pump systems with energy storage for building heating. J Eng Res Appl Sci 2018;7:759–64.
- [225] Stritih U, Zavrl E, Paksoy HO. Energy analysis and carbon saving potential of a complex heating system with solar assisted heat pump and phase change material (PCM) thermal storage in different climatic conditions. Euro J Sustain Develop Res 2019:3:em0067.
- [226] Fan CC, Yan G, Yu JL. Thermodynamic analysis of a modified solar assisted ejector-compression heat pump cycle with zeotropic mixture R290/R600a. Appl Therm Eng 2019;150;42–9.
- [227] Chen JH, Yu JL. Energy and exergy analysis of a new direct-expansion solar assisted vapor injection heat pump cycle with subcooler for water heater. Sol Energy 2018;171:613–20.
- [228] Chen JH, Yu JL, Qian SX. Subcooling control method for the adjustable ejector in the direct expansion solar assisted ejector-compression heat pump water heater. Appl Therm Eng 2019;148:662–73.
- [229] Fraga C, Hollmuller P, Mermoud F, Lachal B. Solar assisted heat pump system for multifamily buildings: Towards a seasonal performance factor of 57 Numerical sensitivity analysis based on a monitored case study. Sol Energy 2017;146: 543-64

- [230] Duarte WM, Paulino TF, Pabon JJG, Sawalha S, Machado L. Refrigerants selection for a direct expansion solar assisted heat pump for domestic hot water. Sol Energy 2019;184:527–38.
- [231] Ran SY, Li XT, Xu W, Wang BL. A solar-air hybrid source heat pump for space heating and domestic hot water. Sol Energy 2020;199:347–59.
- [232] Paulino TF, Oliveira RN, Maia AAT, Palm B, Machado L. Modeling and experimental analysis of the solar radiation in a CO2 direct-expansion solarassisted heat pump. Appl Therm Eng 2019;148:160–72.
- [233] Wang YQ, Rao ZH, Liu JX, Liao SM. An optimized control strategy for integrated solar and air-source heat pump water heating system with cascade storage tanks. Energy Buildings 2020;210:109766.
- [234] Paradeshi L, Srinivas M, Jayaraj S. Performance studies of R433A in a direct expansion solar-assisted heat pump. Int J Ambient Energy 2020;41:262–73.
- [235] Li FL, Chang Z, Li XC, Tian Q. Energy and exergy analyses of a solar-driven ejector-cascade heat pump cycle. Energy 2018;165:419–31.
- [236] Lee SJ, Shon BH, Jung CW, Kang YT. A novel type solar assisted heat pump using a low GWP refrigerant (R1233zd(E)) with the flexible solar collector. Energy 2018:149:386–96.
- [237] Cao Y, Mihardjob LWW, Parikhanic T. Thermal performance, parametric analysis, and multi-objective optimization of a direct-expansion solar-assisted heat pump water heater using NSGA-II and decision makings. Appl Therm Eng 2020;181: 115892.
- [238] Liu M, He YE, Zhang HF, Su H, Zhang ZW. The feasibility of solar thermal-air source heat pump water heaters in renewable energy shortage regions. Energy 2020:197:117189.
- [239] Han ZW, Bai CG, Ma X, Li B, Hu HH. Study on the performance of solar-assisted transcritical CO2 heat pump system with phase change energy storage suitable for rural houses. Sol Energy 2018;174:45–54.
- [240] Li YH, Kao WC. Taguchi optimization of solar thermal and heat pump combi systems under five distinct climatic conditions. Appl Therm Eng 2018;133: 283–97.
- [241] Vega J, Cuevas C. Parallel vs series configurations in combined solar and heat pump systems: a control system analysis. Appl Therm Eng 2020;166:114650.
- [242] Rabelo SN, Paulino TF, Machado L, Duarte WM. Economic analysis and design optimization of a direct expansion solar assisted heat pump. Sol Energy 2019;188: 164–74.
- [243] Liu ZJ, Wang QM, Wu D, Zhang YL, Yin H, Yu HC, et al. Operating performance of a solar/air-dual source heat pump system under various refrigerant flow rates and distributions. Appl Therm Eng 2020;178:115631.
- [244] Youssef W, Ge YT, Tassou SA. Indirect expansion solar assisted heat pump system for hot water production with latent heat storage and applicable control strategy. Energy Procedia 2017;123:180–7.
- [245] Ma JL, Fung AS, Brands M, Juan N, Moyeed OMA. Performance analysis of indirect-expansion solar assisted heat pump using CO2 as refrigerant for space heating in cold climate. Sol Energy 2020;208:195–205.
- [246] Rabelo SN, Paulino TF, Duarte WM, Maia AAT, Machado L. Experimental analysis of the influence of the expansion valve opening on the performance of the small size CO2 solar assisted heat pump. Sol Energy 2019;190:255–63.
- [247] Wei B, Wang YZ, Liu ZJ, Liu BX. Optimization study on a solar-assisted air source heat pump system with energy storage based on the economics method. Int J Energy Res 2020;44:2023–36.
- [248] De León-Ruiz JE, Carvajal-Mariscal I. Mathematical thermal modelling of a directexpansion solar-assisted heat pump using multi-objective optimization based on the energy demand. Energies 2018;11:1773.
- [249] Lu J, He GQ, Mao F. Solar seasonal thermal energy storage for space heating in residential buildings: Optimization and comparison with an air-source heat pump. Energy Sources Part B 2020;15:279–96.